ELSEVIER

Chemical Engineering Journal 90 (2002) 3–23

Chemical Engineering Journal

www.elsevier.com/locate/cej

Recent developments on multiscale, hierarchical modeling of chemical reactors

S. Raimondeau [a], D.G. Vlachos [b,*]

[a] *Department of Chemical Engineering, University of Massachusetts-Amherst, Amherst, MA 01003, USA*

[b] *Department of Chemical Engineering and Center for Catalytic Science and Technology, University of Delaware, Newark, DE 19716, USA*

Abstract

A multiscale, hierarchical computational framework is presented for modeling homogeneous–heterogeneous reactors, which exhibit a large disparity in length and time scales. Scales range from quantum, to atomistic, to mesoscopic, to macroscopic. The coupling mechanisms between scales are discussed and illustrated with examples from CO and CH_4 oxidation on platinum. Estimation of reaction mechanism parameters, based on first principle quantum calculations and semi-empirical techniques, is briefly reviewed. These kinetic mechanisms are key input into molecular, continuum, or mesoscopic models. Some emphasis is placed on surface diffusion, which typically falls outside the realm of atomistic models, but it can affect reaction rates and pattern formation on catalytic surfaces. An efficient methodology for parameter optimization of multiscale models is also presented. Finally, we show how mesoscopic models constitute a promising alternative to atomistic Monte Carlo (MC) simulations to account for intermolecular forces, which cannot be properly captured through continuum, mean field (MF) models. Application of these mesoscopic theories to microporous catalysts, such as zeolites, is also discussed.

Keywords: Multiscale; Homogeneous–heterogeneous reactors; Monte Carlo; Mesoscopic modeling; Quantum calculations; Surface diffusion

1. Introduction

Multiscale modeling in chemistry was born in 1913 by David Chapman and advocated by Bodenstein with the introduction of pseudo- or quasi-steady state assumption for intermediate species based on separation of time scales [1]. Related concepts of partial equilibrium (PE) and rate-determining step (RDS) are still often employed in deriving rate expressions of surface kinetics. Mathematically, large activation energy asymptotics and perturbation techniques in general, based on a small parameter, have been used for decades to simplify transport (boundary layer) and kinetics equations that extend over multiple scales [2]. Flame modeling is an example of an area where both chemistry and transport simplifications have been extensively used [3]. Computationally, adaptive mesh refinement is often employed to resolve fine scales in processes with large disparity in length scales whereas techniques, such as implicit solvers and operator splitting, have been developed to deal with stiffness of differential equations [4,5]. A common feature of all these inherently multiscale problems is that they have been treated within a unifying framework of continuum equations of change. While such equations have served well numerous engineering applications, they are often severely limited in predictability or they are even structurally wrong as they neglect or treat phenomenologically phenomena related to intermolecular forces, defects, phase transformations, and so on [6].

The leap in computational power and numerical algorithms enable a new multiscale reactor modeling paradigm that goes beyond the simple separation of time and length scales of continuum equations of change. In this new framework, different scales are modeled using different modeling approaches and tools (a hybrid approach), which are traditionally handled by groups having different research expertise [7–9]. Examples include coupling of discrete molecular modeling, such as molecular dynamics (MD) and stochastic Monte Carlo (MC) simulations, with continuum equations of change for macroscopic scales [10,11]. Accurate parameterization of molecular models demands information about potential energy surfaces to extract intermolecular forces and/or kinetic parameters. This information can be deduced from various quantum mechanical and statistical mechanics calculations (e.g. ab initio, density functional theory (DFT), transition state theory (TST)), depending on accuracy and computational cost. Aside from the quantum, molecular, and continuum scales and models, phenomena in catalytic (and other) chemical reactors often occur at large enough length and time scales, which fall outside the realm of

* Corresponding author. Tel.: +1-302-831-2830; fax: +1-302-831-1048.
E-mail address: vlachos@che.udel.edu (D.G. Vlachos).

1385-8947/02/$ – see front matter
PII: S1385-8947(02)00065-7

Nomenclature

a, b	medium indicator terms
d	diffusion coefficient at high (infinite) temperature
D	diffusion coefficient
Dg_i	gas-phase dissociation energy of species i
E	activation energy
J	interaction potential in a homogeneous medium
k	Boltzmann constant
K	intermolecular potential of adsorbate–adsorbate (lateral) interactions
k_i	rate constant for ith reaction type
p	probability
P	reactant partial pressure
Q_i	heat of chemisorption of species i
r, r'	distances
t	time
T	temperature
u	dimensionless concentration (coverage)
U_0	energy associated with the binding to the catalyst
W	transition probability per unit time
x	macroscopic space variable
y	microscopic space variable
Y	periodic domain

Greek symbols

α, β	surface configurations
δ	Kronecker function
ΔH_{rxn}	heat of reaction
Ω	domain

Subscripts

a	adsorption
b	backward
d	desorption
f	forward
o	leading order term in the Taylor expansion
r	reaction

Superscript

eff	effective

molecular models, but for which continuum constitutive equations are lacking. This intermediate, vaguely understood regime is often called the mesoscale and imposes major challenges because a suitable mathematical and computational framework for such scales was till recently lacking.

The ultimate goal of this new multiscale framework is unprecedented accuracy and the potential of having predictive capabilities from first principles without relying on any fitting or experimental input. Both aspects are key in guiding future experiments and enabling rational design and model-based control of reactions and structures at the molecular level. While, we are currently far from such goal, work in progress will pave the way toward it.

There are two important classes of multiscale models. The first one encompasses problems where information gathered at the small scale is passed into the next level up (bottom-up approach), i.e. the information flow is uni-directional. In some instances, this is sufficient. As an example, ab initio calculation of reaction rate constants of gas-phase reactions as functions of pressure and temperature requires no further knowledge from the reactor scale. Flame and gas-phase CVD models are applications where uni-directional coupling has been practiced. The second class encompasses problems where strong coupling between scales exists, so information flow should be bi-directional. Most homogeneous–heterogeneous reactors fall in this latter class, which is also the focus of this paper. As we discuss later, this flow of information imposes challenges, as robust and efficient numerical algorithms for their solution are still at embryonic stages.

Currently there is explosive growth in multiscale modeling, especially in the area of materials [12–21]. Here we focus on catalytic reactors and discuss ideas mainly from our own work. Specifically, we develop and apply ideas to an important class of reactions, namely oxidation chemistry on noble metals. Major applications entail partial oxidation (e.g. natural gas to syngas), catalytic combustion (e.g. natural gas burning in gas turbines) for energy generation, and end of the pipe treatment of pollutants/waste (e.g. automotive catalytic converter) [22–24].

While these chemistries and reactors exhibit challenging multiscale aspects, they are at the same time some of the simplest catalytic reactors with coupling between all scales. One reason for such simplicity is that oxidation chemistry is fast and often requires low surface area to avoid deep oxidation to complete combustion products. Thus, supported catalysts may not be necessary. Commercial examples include the NH_3 oxidation (Ostwald process) and the HCN formation (Andrussow process) over gauzes [24]. Partial oxidation of CH_4 to syngas over gauzes and low surface area monoliths is another example [25]. Furthermore, in some of these reactors (e.g. monoliths), flows are laminar. These aspects eliminate internal mass transfer modeling and simplify external mass transfer simulations. As a result, these systems exhibit an analogy to high pressure modeling of CVD reactors for growth of films, when the continuum approximation is still valid. Figs. 1 and 2 depict typical length and time scales, respectively, in such a relatively simple chemical reactor for the oxidation of CO on platinum.

The overall hierarchical multiscale approach we discuss in this paper is depicted in Fig. 3. The specific organization of this paper is as follows. First, we discuss chemistry advances and limitations and provide examples from CO and CH_4 reactions on platinum. Next, we discuss the surface simulator, i.e. modeling techniques of surface processes. Some emphasis is placed on surface diffusion that is particularly

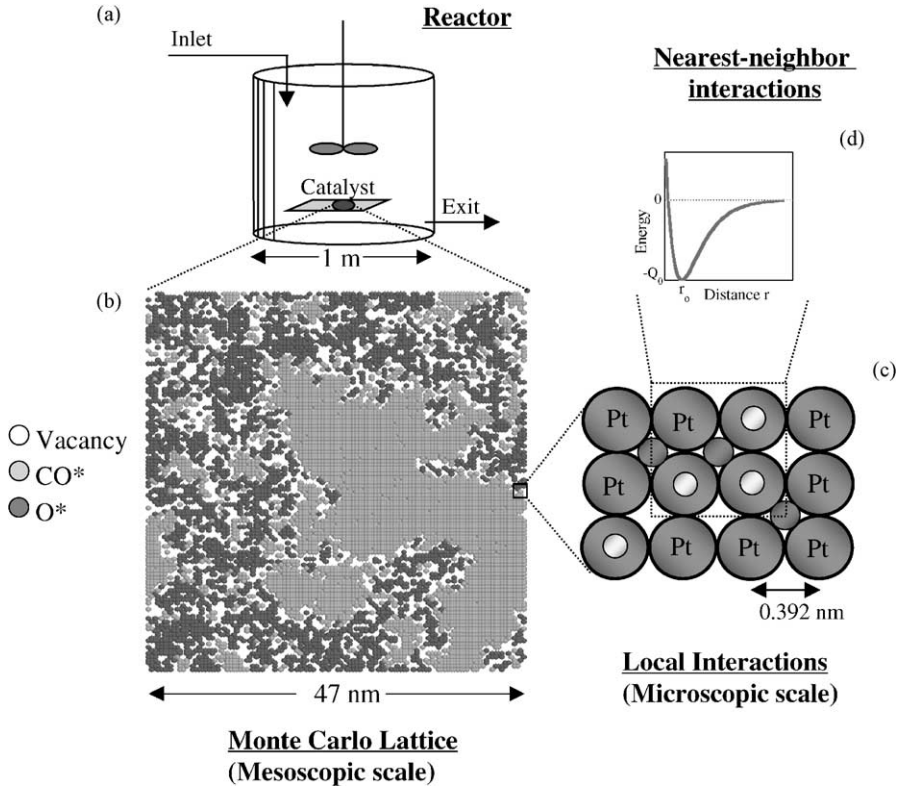

Fig. 1. Length scales involved in the oxidation of CO on a platinum(1 0 0) surface embedded in a CSTR at atmospheric pressure (a); snapshot from a MC simulation, illustrating the distribution of adsorbates (b); schematic of atomic species (O*) adsorbed on hollow sites and the molecular species (CO*) adsorbed on on-top sites (c); schematic of interactions in the BOC framework which are described using a Morse potential (d).

challenging to capture with molecular models. Coupling of quantum and molecular as well as molecular and continuum scales is illustrated. Optimization of parameters of molecular and multiscale models is also discussed. Finally, extension of molecular scale models to mesoscales is briefly touched upon.

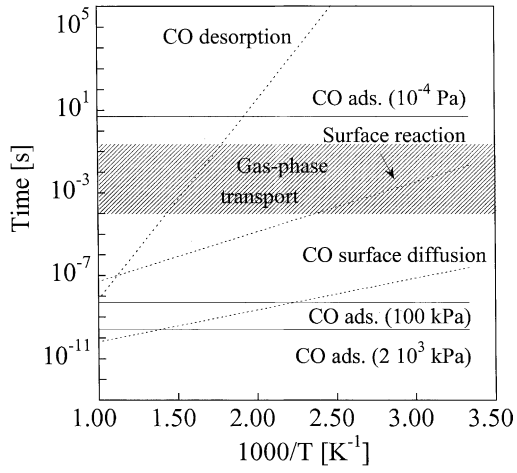

Fig. 2. Time scales of selected steps from the oxidation of CO on platinum vs. inverse temperature. CO adsorption is non-activated but depends on pressure. Typical gas-phase transport time scales are indicated for short contact time reactors. The surface diffusion of CO can be orders of magnitude faster than the other processes. The value of diffusivity was taken from [75], whereas the rest of the time scales were computed using columns 8 and 9 of Table 1, on a clean surface (zero-coverage limit).

2. Advances and limitations of chemistry

Due to the advance of ab initio methods and computational power as well as advanced experimental techniques, gas-phase chemistry is considerably more mature than solution and surface chemistries. Detailed gas-phase reaction mechanisms are therefore commonly used in flames, atmospheric chemistry, and CVD modeling. Next we discuss each type of chemistry, focusing mainly on oxidation chemistry.

2.1. Gas-phase reactions

Gas-phase oxidation reactions are a prototype example of radical based chemistry. They typically exhibit higher activation energies than their counterparts on noble metals, and thus, they can be left out in relatively low temperature processes modeling (e.g. catalytic converter). However, in both catalytic combustion and partial oxidation, pressure and temperatures are high, so gas-phase reactions should be included. Their onset is either desirable (e.g. in gas turbines and some partial oxidation processes [26]) or not (e.g. due to explosions and degradation of selectivities of some partial

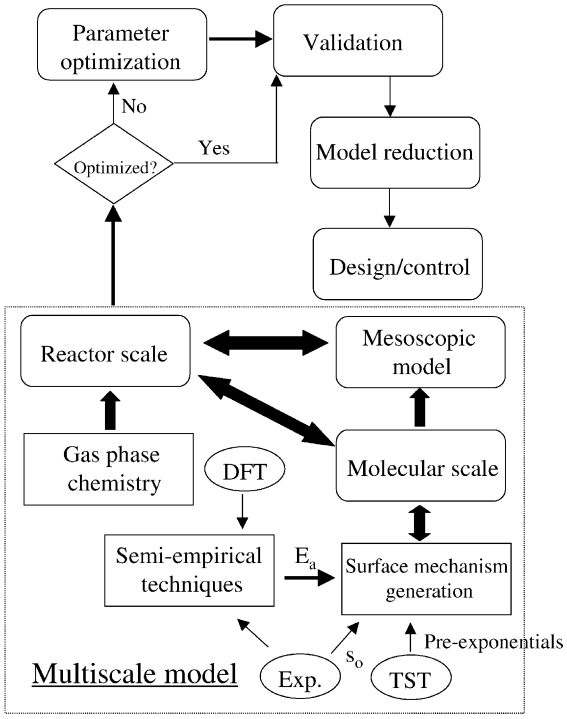

Fig. 3. Overall multiscale approach discussed in this paper. The multiscale model includes a surface simulator coupled with a gas-phase simulator and the corresponding reaction mechanisms as input. A mesoscopic model can replace molecular models in order to simulate larger time and length scales of the surface. Design and control of homogeneous–heterogeneous reactors with molecular resolution are ultimate goals of such models.

oxidation processes). While power law rate expressions are occasionally used, the development of CHEMKIN suit of tools [27–29] has catalyzed the widespread use of detailed reaction mechanisms.

For gas-phase chemistry, we usually employ a version from the Gas Research Institute (GRI) mechanisms available on the web [30]. This mechanism is heavily optimized against a variety of experimental data, reactors, and molecules encountered in natural gas combustion. The most recent version includes 325 reactions among 53 species.

2.2. Surface chemistry

In contrast to gas-phase chemistry, surface chemistry has been less well-developed and has followed the schematic shown below. One-step chemistry is often employed, where the reaction rate is fitted to experimental data. In other cases, this rate expression is based on Langmuir–Hinshelwood kinetics and derived using reduction ideas based on a RDS. Finally, detailed reaction mechanisms for small molecules, such as CO oxidation and NH_3 synthesis, are common as well. An example is given in Table 1 for the CO oxidation on platinum. Microkinetic analysis emphasized by Dumesic and co-workers [31], where no assumptions about a RDS are employed, has been a significant step toward detailed modeling, but it has slowly been integrated in teaching and research over the last decade. For all practical purposes, surface chemistry has been modeled using the mean field (MF) approximation, where it is assumed

Table 1
Reaction mechanism for the CO oxidation on platinum and selected kinetic parameters from the literature

Reaction	[75] [a]		[140] [b]		[45] [c]		[80] [d]	
	Pre-factor	E_a	Pre-factor	E_a	Pre-factor	E_a	Pre-factor	E_a
$O_2 + 2^* \rightarrow 2O^*$	0.06	0.0	0.003	0.0	0.1	0.0	0.09	0.0
$2O^* \rightarrow O_2 + 2^*$	–	–	5×10^{12}	217.7	1×10^{13}	213.5	1×10^{13}	213.5
$CO + ^* \rightarrow CO^*$	0.84	0.0	0.84	0.0	0.89	0.0	0.89	0.0
$CO^* \rightarrow CO + ^*$	1.25×10^{15}	146.1	1×10^{13}	125.6	9.4×10^{16}	184.2	5.82×10^{17}	184.2
$CO^* + O^* \rightarrow CO_2 + 2^*$	1.645×10^{14}	100.9	1×10^{15}	100.5	–	–	4.9×10^{09}	46.0
$CO_2{}^* + ^* \rightarrow CO^* + O^*$	–	–	–	–	1×10^{11}	79.5	–	–
$CO^* + O^* \rightarrow CO_2{}^* + ^*$	–	–	–	–	4.9×10^{09}	46.0	–	–
$CO_2 + ^* \rightarrow CO_2{}^*$	–	–	–	–	1.0	0.0	–	–
$CO_2{}^* \rightarrow CO_2 + ^*$	–	–	–	–	1×10^{11}	71.2	–	–
$O + ^* \rightarrow O^*$	–	–	–	–	1.0	0.0	–	–
$O^* \rightarrow O + ^*$	–	–	–	–	1×10^{13}	387.7	–	–
$C^* + O^* \rightarrow CO^* + ^*$	–	–	5×10^{13}	62.8	–	–	–	–
$CO^* + ^* \rightarrow C^* + O^*$	–	–	1×10^{11}	184.2	–	–	–	–

The desorption of CO, which is, in general, a key step for predicting experimental results shows large deviations between mechanisms. The pre-factors correspond to sticking coefficients for adsorption steps or pre-exponentials in s^{-1}. Activation energies are in kJ/mol. The symbol "–" indicates that this step was not included in the reaction mechanism.

[a] Kinetic parameters for CO oxidation on Pt(1 1 1).

[b] Kinetic parameters extracted from a methane reaction set fitted to selectivity data of short contact time microreactors.

[c] Kinetic parameters optimized against ignition temperatures at high pressures and reaction rate data under vacuum conditions using a continuum, MF based model.

[d] Kinetic parameters optimized with respect to reaction rates on a Pt(1 0 0) surface under vacuum conditions using a MC simulator (see text).

that adsorbates are homogeneously distributed on the catalyst surface.

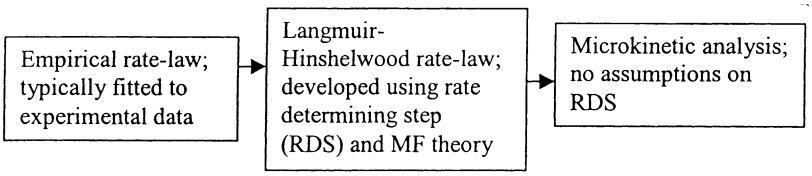

Surface chemistry of small molecules has been implemented manually. However, computational tools have been developed for automatic generation of reaction mechanisms for both gas and surface reactions [32–38]. Independent of the technique used for reaction mechanism generation, estimation of kinetic parameters still remains a challenge.

2.3. Surface chemistry parameter estimation

Parameters of elementary steps are often borrowed from surface science experiments whenever available, and the missing (a few) parameters are fitted to a single set of experiments. Parameters for CO oxidation on platinum, from different literature sources, are given in Table 1. Note that the parameters can differ substantially, especially those in the CO desorption step. As a result, these mechanisms are often inadequate to be predictive over a wide range of conditions or to describe different type of experiments. In addition, for larger molecules, parameters of elementary steps are unknown. This situation is further complicated by the long-standing problem of materials and pressure gaps, which have often limited the integration of experiments under ultra high vacuum on single crystals to practical catalysts and catalytic reactor conditions. Thermodynamic inconsistencies are possible too (for a more detailed discussion see [39]).

As an example, Table 2 shows predictions of the ignition-extinction for CH_4/O_2 mixtures simulated in a stagnation flow reactor, where the flow impinges on a platinum foil for given strain rate indicating an inverse residence time [40] using three literature reaction mechanisms containing of the order of twenty reactions. Two of the mechanisms [41,42] predict ignition temperatures in close agreement to experimental data as they have been tuned for this purpose. However, their predictions for the depicted extinction temperature and the selectivity to syngas (not shown) are poor compared to experimental data. The third mechanism [43] predicts reasonable selectivities (not shown) but a premature ignition at very low temperature and with almost no pre-heating. All three mechanisms assume either explicitly or implicitly that dissociation of methane to carbon follows a pyrolytic path, where the first-step is the RDS, and therefore one can lump the chemistry into a single-step, $CH_4 \rightarrow C + 4H$. Additional examples of reaction mechanism limitations for H_2 and CO oxidation are given in [39,44,45].

There have been a few systematic approaches for parameter estimation when large molecules and reaction networks are modeled. Some are empirical in nature. The Polanyi free energy relationship is a common approach for activation energy estimation from the heat of reaction, with pre-exponentials of homologous series fitted to experimental data [36,46]. The single event approach of Froment has also proved useful [47,48].

At the other end of the spectrum, fundamental quantum chemical computational methods are employed, with DFT being the most popular one for surface processes [49–51]. DFT can be directly used to compute activation energies. However, its computational cost currently prohibits its application to large reaction mechanisms and its on-the-fly use. Therefore, DFT has been mainly used to provide insight into reaction paths. Note that it is easier to compute binding energies than activation energies of surface reactions using DFT. This is an important issue in coupling DFT calculations with semi-empirical techniques discussed next.

The lack of thermodynamic data bases for computing heats of reactions (needed in the Polanyi relationship) and equilibrium constants, and the high concentration of adsorbates at high pressures and/or lower temperatures demands an understanding of the role of adsorbate–adsorbate interactions (both direct and catalyst mediated) in the parameters of surface reactions. Coverage dependent activation energies of desorption are common, but this is not the case for surface reaction steps. We believe that in many instances large discrepancies in reported activation energies are due to different adsorbate concentrations on the surface

Table 2
Comparison of ignition and extinction temperatures predicted using three literature surface reaction mechanisms vs. experimental data in a stagnation flow reactor for 10% methane in air, a strain rate of $10\,s^{-1}$, a heat loss of $4.187\,J/m^2\,K\,s$, and a surface emissivity of 0.15

	Ignition temperature (K)	Power applied at ignition ($J/m^2\,s$)	Extinction temperature (K)	Power applied at extinction ($J/m^2\,s$)
Experimental	845	–	1000	–
[41]	832	11305	805	−12980
[141]	790	12561	605	−19679
[43]	491	2512	992	−17167

The power supply to the surface is also indicated at ignition and extinction. None of the proposed mechanisms is able to predict accurately both ignition and extinction temperatures. Significant variation in power supply is also observed.

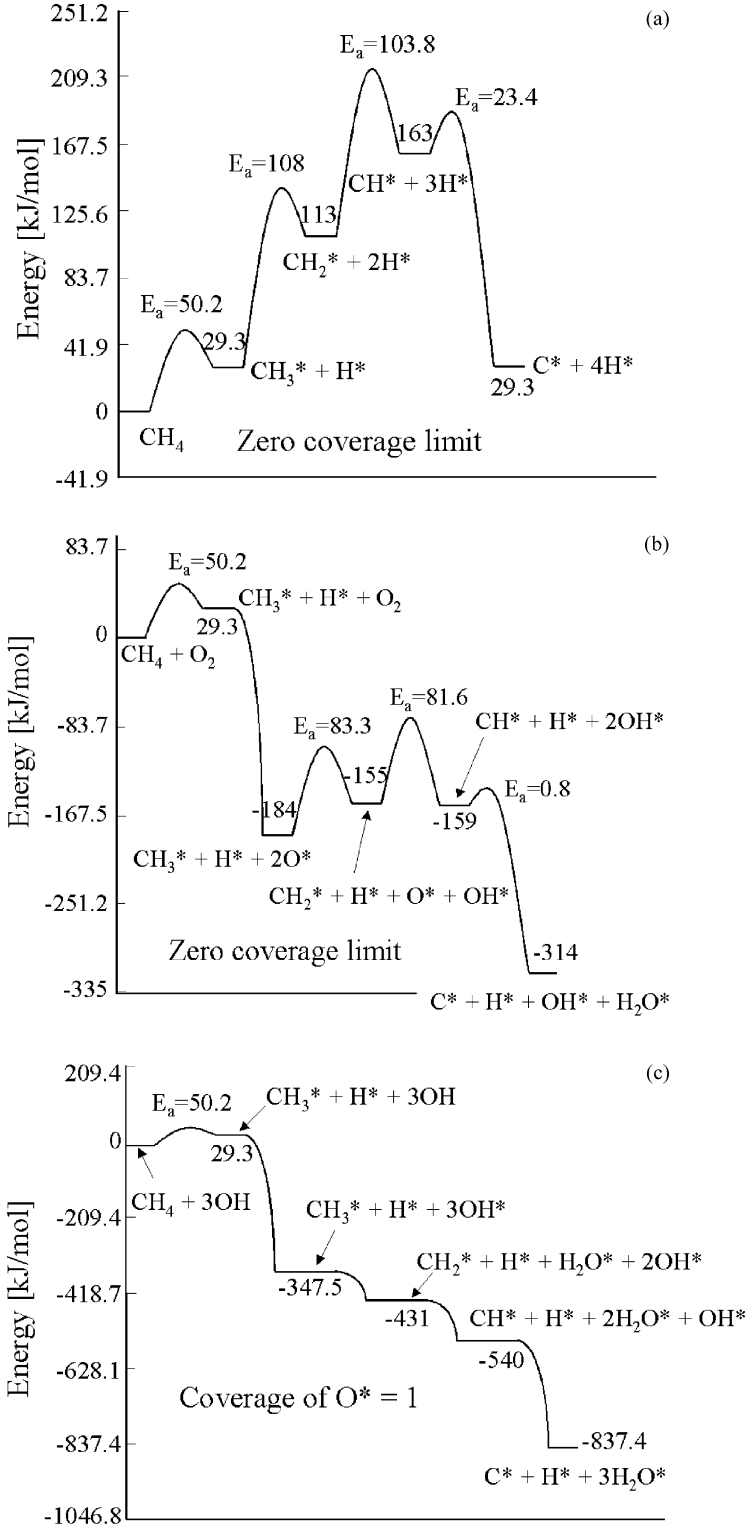

Fig. 4. Energy diagrams for methane decomposition on platinum through the pyrolytic path (a); an oxygen-assisted path (at the zero-coverage limit) corresponding to one CH_4 molecule reacting with an O_2 molecule (b); and an oxygen-assisted path on an oxygen-rich surface ($\theta_{O^*} \rightarrow 1$) (c) as predicted using the BOC formalism [54]. The different energy levels indicate that the presence of oxygen promotes methane dissociation. Adsorbate–adsorbate interactions strongly modify the potential energy surface. MF theory is used to account for the coverage dependence of energetics.

encountered in different experiments (see examples and discussion in [39]). Furthermore, the opportunity to improve accuracy of empirical methods using quantum chemical simulations, for at least small and medium size molecules, stimulates the use of suitable semi-empirical techniques. One such technique is the bond order conservation (BOC) or unity bond index–quadratic exponential potential (UBI–QEP).

BOC method was developed by Shustorovich and co-workers [52,53] and applied to derive heats of reactions and activation energies of reaction pathways for a wide variety of reaction systems, [53]. Despite its semi-empirical nature, good agreement (often within 2–4 kcal/mol) with experiments is obtained. However, its use in performing quantitative reactor model calculations has not been attempted till recently [39]. Next, we discuss activation energy estimation using the BOC, and the coupling between BOC to MC and quantum (DFT) simulations will follow in the next section.

2.3.1. Prediction of activation energies using BOC

A major advantage of the BOC method is the use of analytical expressions to estimate activation energies of different types of reactions using only heats of chemisorption and gas-phase dissociation energies as input. These expressions are obtained through an energy minimization of the interaction of a two-center metal-adsorbate entity described by a Morse potential. The entire framework relies on the fundamental assumption of conservation and pairwise-additivity of bond-order describing all interacting two-center bonds.

As an example, to compute the zero-coverage forward and backward activation energies of the surface reaction $CH_3{}^* + {}^* \rightarrow CH_2{}^* + H^*$, the following semi-empirical, analytical formulae are used

$$\Delta H_{\mathrm{rxn}} = D\mathrm{g}_{\mathrm{CH_2-H}} + Q_{\mathrm{CH_3}} - Q_{\mathrm{CH_2}} - Q_{\mathrm{H}} \quad (1)$$

$$E_{\mathrm{f}} = \frac{1}{2}\left(\Delta H_{\mathrm{rxn}} + \frac{Q_{\mathrm{CH_2}} Q_{\mathrm{H}}}{Q_{\mathrm{CH_2}} + Q_{\mathrm{H}}}\right) \quad (2)$$

$$E_{\mathrm{b}} = E_{\mathrm{f}} - \Delta H_{\mathrm{rxn}} \quad (3)$$

where Q_i is the heat of chemisorption of species i, $D\mathrm{g}_{\mathrm{CH_2-H}}$ the gas-phase dissociation energy, ΔH_{rxn} the heat of reaction, E_{f} the forward activation energy, and E_{b} is the backward activation energy. We obtain $E_{\mathrm{f}} = 107.8$ kJ/mol and $E_{\mathrm{b}} = 25.9$ kJ/mol at zero-coverage with $D\mathrm{g}_{\mathrm{CH_2-H}} = 259.6$ kJ/mol, $Q_{\mathrm{CH_3}} = 159.1$ kJ/mol, $Q_{\mathrm{CH_2}} = 284.7$ kJ/mol, and $Q_{\mathrm{H}} = 252.1$ kJ/mol.

The binding energies, used as an input to the BOC framework, can be obtained experimentally (e.g. using microcalorimetry, adsorption isotherms, or temperature programmed desorption), estimated theoretically, or derived from DFT calculations. Lateral interactions can be also taken into account [52,53], and thus, coverage-dependent activation energies can be obtained from coverage-dependent heats of chemisorption. Since reaction mechanisms of moderate size or large molecules typically consist of many more steps than species, calculation of binding energies with DFT is a much easier and computational tractable task. To illustrate this point, we refer to a newly developed C1 surface reaction mechanism for methane oxidation on platinum that consists of 62 irreversible reactions but only 10 species [54].

As an example, Fig. 4 depicts illustrative energy diagrams for methane decomposition on platinum. The pyrolytic decomposition path exhibits the highest activation energies in intermediate steps, contradicting the literature hypothesis of single-step decomposition. Oxygen-assisted paths, either through O or OH, exhibit lower activation energies, especially on an oxygen-covered surface. Based on energetics alone, one can conclude that oxygen assists methane dissociation. Transient experiments in our lab have indeed qualitatively confirmed this prediction [25]. However, caution should be exercised in inferring the RDS based solely on energetics. For example, reactor scale simulations for methane oxidation indicate that the preferred path changes with operating conditions of temperature, composition, etc. [54].

2.3.2. Values of pre-factors: sticking coefficients and pre-exponentials

First principles computation of kinetic pre-factors is possible either through MD [53] for low activation energy (fast) processes or TST for high activation energy (slow) processes. However, these approaches can be quite computationally involved. Furthermore, there are uncertainties in microscopic rate constants associated with errors in activation energies, the presence of defects, catalyst aging, and adsorbate–adsorbate interactions, which cannot be easily or accurately accounted for. While this is an area where more research will be valuable, in the interim we propose to simply obtain order of magnitude of sticking coefficients, from surface science experiments of major species, whenever available, and TST estimates of pre-exponentials based on the type of reaction [31]. This procedure provides a screening mechanism for semi-quantitative comparison to experimental data. Subsequently, refinement of important pre-factors can be carried out through a multistep optimization procedure discussed later. This mechanism can be used to propose experiments for further validation and investigate the effect of previously unexplored reaction paths on reaction rates and concentrations.

3. Surface simulator

The surface mechanism and the corresponding kinetic parameters represent the major input to a surface simulator. Such input entails knowledge about the elementary, microscopic steps (reaction and diffusion paths), the corresponding pre-factors, namely pre-exponentials and sticking coefficients, and the activation energies.

The conventional approach in modeling catalytic reactors entails continuum equations of change for surface processes. Under the MF assumption, ordinary differential equations

suffice to study dynamics and algebraic equations are adequate for steady state situations. In order to study pattern formation on catalytic surfaces, the MF assumption is relaxed, and continuum diffusion-reaction (partial differential) equations are employed [55].

The inability of MF models to accurately treat spatial effects at the molecular level and phenomena such as nucleation and coalescence of clusters of adsorbates, uphill surface diffusion, etc. has led to the development of an hierarchy of alternative surface simulators. Some examples include the Bragg–Williams approximation, the Bethe–Peierls and the modified Bethe approximations, the Kukuchi cluster approximation, and the quasi-chemical approximation listed in [56]. At the top of the hierarchy lay MC simulations [57–59], which have been by far the most popular surface simulators over the last 15 years and are discussed next.

3.1. Monte Carlo simulations

MC simulations were introduced by Wicke et al. [60] and a few years later by Ziff et al. [61] who studied CO oxidation on platinum. Ziff's work and subsequent studies focused primarily on phase transitions and critical exponents of this new, exciting class of non-equilibrium statistical mechanical systems. A burst in activity on more complex kinetic systems and investigation of the role of various features such as desorption, Fickian surface diffusion, defects, and adsorbate–adsorbate interactions in phase transitions appeared after Ziff's work [62]. In parallel, significant developments in algorithms have been also achieved, including the implementation of real time [62–69], the elimination of null events [67–69], the implementation of generic codes for treating complex surface reaction mechanisms, etc. For a review of MC algorithms and their application to different physical systems, see [62,70–76]. The work presented here uses an efficient continuous time MC method with lists of neighbors and local update discussed in detail in [69]. Recently, there is more emphasis on implementing realistic kinetic parameters in MC simulations enabling comparison of macroscopic features (e.g. reaction rates) with experimental data [77–80].

In MC simulations of surface reactions, one typically maps catalyst sites on a lattice on which adsorbates reside. Such an approach belongs to the general class of interacting particle system (IPS), which describe cooperative phenomena, with Ising models being a well-known example from magnetism. A snapshot of a MC simulation on a square lattice representing the Pt(1 0 0) surface is shown in Fig. 1b. MC simulations provide the exact, stochastic solution to the time-dependent master equation describing the surface processes

$$\frac{\mathrm{d}p_\alpha}{\mathrm{d}t} = \sum_\beta \left[W_{\alpha\beta} p_\beta - W_{\beta\alpha} p_\alpha \right] \tag{4}$$

where p_α is the probability of the surface being in configuration α and $W_{\alpha\beta}$ the transition probability per unit time of the surface going from configuration β to α. As a discrete technique, it takes into account local effects in the various probabilities, such as the presence of point or small clusters of defects, short-range adsorbate–adsorbate interactions, the necessity for proximity (adjacency) of sites for dissociative adsorption and bimolecular reactions, and so on. These small length scale inhomogeneities, depicted in Fig. 1b, are features typically not treated accurately by MF models.

With this input (discussed in the chemistry section), transition probabilities can be computed for a large class of cases in [69], in a straightforward manner in order to determine the spatio-temporal evolution of the catalytic surface, i.e. a MC simulation should be thought of as a sophisticated solver of surface kinetics with atomic spatial resolution but extreme computational cost. However, the fundamental physics and chemistry of the problem are incorporated in the microscopic events modeled and their associated transition probabilities. Identification of important events/paths can be achieved through MD and/or experiments. From the resulting distribution of the adsorbed species on the catalytic surface, spatial and temporal average (homogenized) properties can be derived, such as coverages and reaction rates, which are of practical interest.

3.2. Surface diffusion

Several experimental techniques, such as field emission microscopy (FEM), field ion microscopy (FIM), laser-induced thermal desorption (LITD), and scanning tunneling microscopy (STM) [81,82] are used to study surface diffusion (diffusion coefficients, atom clustering, kinetics, etc.). From these studies, it can be inferred that realistic surface diffusion cannot be practically run with MC or multiscale simulations as its corresponding transition probability is usually several orders of magnitude higher than those of the rest microprocesses (see Fig. 2 for an example). Consequently, MC simulations are typically considered as the zero (or very slow) diffusion limit and MF calculations as the infinite Fickian diffusion limit. Obviously, this situation limits the possibility of comparing molecular and multiscale simulators to experimental data for conditions where surface diffusion is important.

In order to study the effect of surface diffusion on surface kinetics, several approximate techniques have been proposed. For example, in [83–85] the catalytic surface was equilibrated by allowing a certain number of surface diffusion events between each successful microprocess for different microscopic diffusion dynamics. Similar ideas were explored in the CO oxidation on Pd(1 0 0) [86] and in a study on the effect of surface diffusion on TPD data [84], where quasi-equilibrium was observed at sufficiently fast diffusion rates. A hybrid approach has also been implemented, where the immobile adsorbate was described using a MC technique, and the mobile species was solved using a MF approximation [86,87]. In this technique, a uniform distribution of the mobile species on the remaining vacant

sites was assumed [87] that can be corrected to include adsorbate–adsorbate interactions through the Bethe–Peierls approximation [86]. Note that in many studies on diffusion, the Metropolis algorithm was employed, where the energy for hopping is simply taken as the difference in binding energy between the departing site and the target site [88], despite the fact that this algorithm does not necessarily capture the correct physics (dynamics) of migration.

Here, similar to some of the aforementioned studies, we propose that in the absence of spatial patterns of relatively large length scale (e.g. several microns), it is possible to obtain the actual reaction rate from MC simulations. To achieve this, surface diffusion is progressively increased until a plateau in the surface reaction rate is reached, indicating that faster diffusion does not further change the overall reaction rate. This asymptotic limit is typically reached when the surface diffusion rate is about three to four orders of magnitude faster than those of the rest processes, a computationally completely feasible situation and consistent with scaling analysis of continuum equations of change. Furthermore, various surface diffusion mechanisms can be explored (e.g. Fickian, non-Fickian, first nearest or further nearest neighbor jumps, Arrhenius dynamics, parabolic jump dynamics, etc.) [81,89].

Fig. 5a gives an example of the asymptotic behavior observed, as the surface diffusion increases, for the case of Fickian CO surface diffusion in the oxidation of CO on platinum. The reaction rates are in kg/m^2 s. The indicated error bars show that as surface diffusion increases, the statistical accuracy diminishes due to the enhanced sampling of surface diffusion compared to the rest processes. It is noted that the fastest diffusion coefficient used in these MC simulations is still several orders of magnitude slower than the actual diffusion coefficient reported in the literature (compare to Fig. 2). The asymptotic value is in good agreement with the MF model for these conditions, which holds for spatially homogeneous adlayers. Snapshots of the adsorbed layer depicted also in Fig. 5 indicate that despite the agreement in

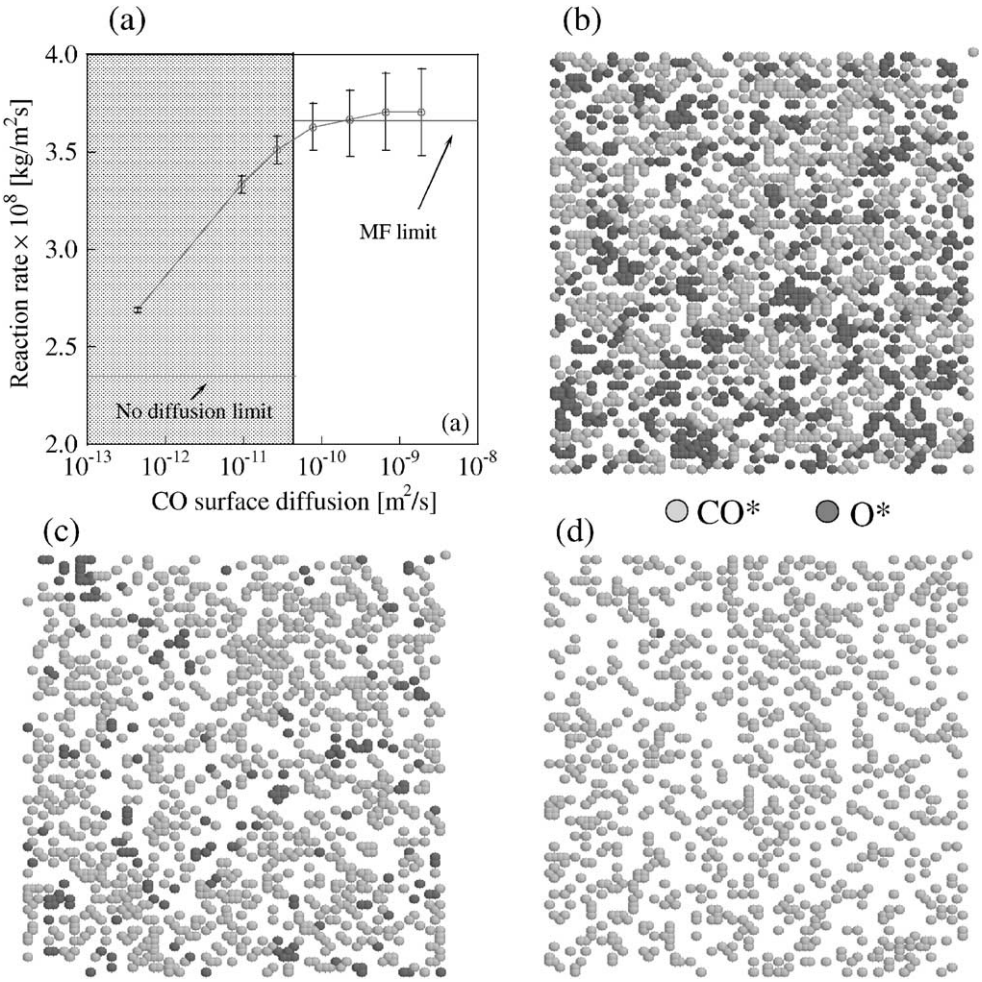

Fig. 5. Reaction rate on a Pt(1 0 0) surface obtained from MC simulations at UHV conditions, as the CO Fickian surface diffusion is gradually increased at partial pressures of $P_{O_2} = 2.66$ nbar and $P_{CO} = 0.4$ nbar for a surface temperature of 475 K (a). No lateral CO*–CO* interactions were included in any step. For sufficiently fast diffusion, a plateau in the reaction rate is reached. Error bars indicate statistics. Snapshots of the catalytic surface for three different conditions: no surface diffusion (b); $D_{CO} = 9.4 \times 10^{-12}$ m^2/s (c); $D_{CO} = 1.9 \times 10^{-9}$ m^2/s (d). The fast surface diffusion simulated does not lead to complete homogenization of the surface. No surface reconstruction was considered.

rate with the MF model, for the fastest diffusion considered here, small islands of CO are still noticeable (lack of complete homogenization).

Since MC simulations with surface diffusion are computationally very demanding, it is useful to know a priori the regimes where surface diffusion is RDS and should not be neglected. To achieve this, two techniques can be employed, namely sensitivity analysis (SA) and PE analysis. SA is a more general but computationally demanding method. In the brute force SA, one increases (e.g. doubles) the rate of surface diffusion and performs a new MC simulation. Surface diffusion is important only when the reaction rate changes. Fig. 5a can be thought of as an example of brute force SA for surface diffusion (more precisely, this a parametric continuation). On the other hand, PE requires no additional MC simulations as it provides information about whether an adsorbed species is in PE and as a result, its surface diffusion is unimportant. This can be done fairly easily by comparing the rates of adsorption, desorption, and reaction of each species as detailed in [90].

The good agreement between MF and MC simulations for moderately fast diffusion raises the question of the need of complex MC surface simulators. Currently, we cannot answer this question comprehensively. By conducting MC under vacuum conditions and multiscale simulations at high pressures, we have found that the agreement between MF and MC simulators holds under many conditions when CO surface diffusion is included. An interesting finding is that the coupling with the gas-phase offers an additional route for homogenization of adsorbates through a desorption–re-adsorption mechanism, and thus, overall the differences between continuum and hybrid simulations are smaller at higher pressures for coupled reactors, even in the absence of surface diffusion. However, deviations have also been found near extinction in both the reaction rates and extinction temperatures. We have attributed this to the fact that surface diffusion of adsorbed O is not considered in MC simulations (since it is too slow) and prior to extinction the non-random distribution of the O adatoms on the surface creates spatial inhomogeneities resulting in differences between the two models [90]. Moreover, when lateral interactions between the CO species are considered, CO diffusion depends on the local distribution of adatoms on the surface (non-Fickian surface diffusion), and non-MF behavior can be found. We will return to this issue in the mesoscopic modeling section.

An important observation is that principles from conceptual process design of chemical processes can be applied to hierarchical multiscale models. In particular, low-level MF, continuum reactor scale simulations can be used as a fast guide in model predictions, sensitivity and PE analyses, and experiment selection for parameter optimization of high level molecular and multiscale models. This input from low-level models into high-level models minimizes the overall computational cost.

3.3. Quantum-molecular coupling

In the idealized case of no adsorbate–adsorbate interactions (both direct and surface mediated), the coupling between quantum and molecular scales is uni-directional. Therefore, one uses DFT or BOC, in conjunction with TST, to store the rate constants in Arrhenius form. This situation parallels gas-phase reactions and reactor scale simulators mentioned in the introduction. Practically, this occurs at the zero-coverage limit (sufficiently low pressures and/or high temperatures). An example of this approach has been recently used [91]. However, the rate of surface processes can be strongly influenced by adsorbate–adsorbate interactions, since the potential energy landscape can be altered by nearby, co-adsorbed species. This is well-known for desorption steps through TPD and microcalorimetry experiments, and has been included in MC simulations, by varying the activation energy of desorption of a species typically as a linear function of the number of its first nearest neighbors. Using BOC, Shustorovich has advocated similar effects for surface reactions, which we illustrate in Fig. 4 for selected oxygen-assisted paths of methane decomposition and for hydrogen oxidation on platinum in [39]. This situation alludes to many body effects in reaction events. Knowledge about the specific distribution of species (microconfigurations) on the catalytic surface is then required to compute energetics. This information is provided from MC simulations, but due to its many body nature, it fluctuates in both time and space. In turn, the activation energies are needed to compute transition probabilities for updating the distribution of species in MC simulations. As a result, the coupling between quantum and molecular scales is bi-directional, an issue that has been downplayed till recently.

For small reaction systems, DFT calculations can be directly coupled with MC simulations. We propose that this can be done by creating a priori a kinetic database (lookup table) by DFT for a small number of different surface microconfigurations, that is then incorporated into the MC simulations. If the number of possible configurations is large, BOC can be first used in MC (as discussed next), and by sampling the most important microconfigurations during a MC simulation, the lookup table can be then created off-line by DFT and incorporated into the MC simulator for future calculations. This idea of a lower-level model assisting a higher-level model parallels again hierarchical process design concepts mentioned earlier.

For more complex reaction mechanisms, DFT is too intensive to currently use even for non-interacting cases. The BOC method presents a feasible alternative to compute the activation energies of all elementary steps within a few kcal/mol. For these systems, the number of local microconfigurations can become very large when all interaction effects are taken into account (different adsorbing sites, direct and indirect interactions, many co-adsorbed species, etc.). When a null event MC algorithm is used, we propose the corresponding activation energies can be computed on the

fly using BOC expressions after a microconfiguration has been selected. On the other hand, when a class or list based algorithm is used, the transition probabilities of all microconfigurations encountered on the surface at that instant are needed. This can result in a large number of possible microconfigurations and a huge database (lookup tables) using the BOC expressions. For this reason, a simplification using single type of sites and taking the heats of chemisorption as functions of the local (discrete) coverage can be pursued [92].

Finally, a hybrid of DFT and BOC is feasible as well. Here the zero-coverage heats of chemisorption are computed by DFT, and adsorbate–adsorbate interactions are modeled through BOC. By taking into account different types of binding sites through analytic formulae, 'first principles MC' simulations can be carried out [78,93] (terminology after Neurock and co-workers).

Diffusion in zeolites is an example where a hierarchy of quantum and molecular models has been recently employed [74,89,94]. Trout and co-workers applied electronic structure methods to calculate thermodynamic parameters for possible elementary reactions in the decomposition of NO_x over Cu-ZSM-5 [95]. Based on these insights, they developed a KMC model of reaction and diffusion in this system, seeking the optimal distribution of isolated reactive Cu centers [96]. This hierarchical approach to realistic modeling of complex systems presents an attractive avenue for future research.

Of all the dynamics studies performed on zeolites, very few have explored the potentially quantum mechanical nature of nuclear motion in nanopores [97–100]. Quantum modeling of proton transfer in zeolites [98,100,101] is relevant in catalytic applications. Such modeling will become more prevalent in the near future, partially because of recent improvements in quantum dynamics approaches [100], but mostly because of novel electronic structure methods developed by Sauer et al. [102,103], which can accurately compute transition state parameters for proton transfer in zeolites by embedding a quantum cluster in a corresponding classical forcefield. To facilitate calculating quantum rates for proton transfer in zeolites, Fermann and Auerbach developed a novel semi-classical TST (SC–TST) for truncated parabolic barriers [100], based on the formulation of Hernandez and Miller [104].

The coupling between quantum calculations, BOC, and MC simulations has been nicely illustrated in the decomposition of NO on Rh(1 0 0) [77,78], ethylene hydrogenation on Pt [77,78,105], and the desorption of O from Rh(1 0 0) [106,107]. The zero-coverage binding energies were computed using DFT calculations and found in very good agreement with experimental data. Due to the large number of DFT computations involved, BOC was used to include the effect of lateral interactions knowing the species distribution on different active sites (on-top, bridge, and hollow) of the catalytic surface from the MC simulation. Furthermore, a scaling (correction) factor was used to match BOC estimates with DFT calculations. Lateral interactions between

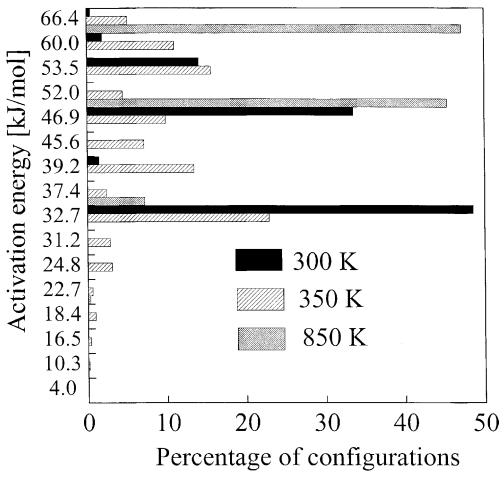

Fig. 6. Distribution of activation energies derived from BOC with single type of site (see text) for the CO surface oxidation reaction on Pt at three temperatures indicated, for $P_{O_2} = 2.66$ nbar and $P_{CO} = 0.4$ nbar. Changes in the population of reaction activation energies is observed, with a broader distribution near ignition at ~350 K.

molecules in the ethylene hydrogenation system were treated as an explicit function derived from extended Huckel theory. Coupling BOC with MC simulations has been also illustrated in a study of the effect of adsorbate interactions in the TPD spectra for CO desorption on Pd(1 0 0) [79] and Ni(1 0 0) [108], and H_2 desorption on Mo(1 0 0) and Ni(1 1 1) [79]. This analysis was extended to include interactions between co-adsorbates using corrected BOC expressions for TPD spectra of CO and H_2 co-adsorbed on Ni(1 0 0) and Rh(1 0 0) [93]. A null event type MC algorithm has been used, and the corrected activation energies were computed on the fly. Good agreement was found with the experimental spectra.

Fig. 6 shows the distribution of activation energies of surface reaction in the catalytic oxidation of CO at three surface temperatures indicated, for $P_{O_2} = 2.66$ nbar and $P_{CO} = 0.4$ nbar. The two low temperatures correspond to situations prior to ignition, whereas the higher temperature corresponds to an ignited catalyst. First-nearest neighbors adsorbate–adsorbate interactions are taken into account through the BOC formalism with a single type of sites in the MC simulator (see methods above and see [39] for continuum models). The heats of chemisorption are taken to depend linearly on the local coverage. Sixteen different activation energies are computed for the corresponding microconfigurations. The distribution of the most probable microconfigurations shifts to higher activation energies with increasing surface temperature. Indeed, the dominant configuration at 300 K on the extinguished branch corresponds to high local coverage of CO* and low local coverage of O*. Near ignition, a broader distribution of microconfigurations is observed as the coverage of O* increases. Under these conditions, the surface is only partially covered with O* species explaining the high activation energy of isolated configurations. Despite the significant variation of the

population of activation energies of surface reaction with varying conditions, there is little influence of such effects on reaction rate for these 'fast' reactions. This surprising result is because the RDS is often adsorption and/or desorption of reactants. It appears then that the surface is 'forgiving' and allows for simple models from the hierarchy. However, for slower reactions this may not be the case.

4. Reactor scale simulator

The input to the gas-phase simulator includes the gas-phase chemistry, constitutive equations for transport, thermodynamic and transport parameters, an equation of state, and adsorption–desorption rates from the surface simulator. These surface-related rates are encountered either in the conservation equations, for lumped systems (e.g. a catalytic CSTR, a PFR with catalyst at the wall (film reactor) and perfect mixing in the radial direction), or the boundary conditions of distributed systems (e.g. a stagnation flow reactor). As a result, coupling is bi-directional. The surface simulator provides these rates.

Following [109], the equations of change have been well established. With the development of advanced computational fluid dynamics (CFD) software, such as Fluent and CFX, modeling of laminar flows has advanced considerably in recent years, and we will not attempt to cover this topic here. It is worth though mentioning that the integration of complex reaction mechanisms with fluid flow is still limited mainly to one-dimensional reacting (e.g. stagnation) flows [42,110]. Two-dimensional reacting flow simulations with complex chemistry are becoming more common but are still non-trivial in computational resources and numerical challenges [111–115]. An exception to this rule has been the CVD modeling, where the decoupling of mass transfer from fluid and heat transfer has enabled one over the last decade to carry complex chemistry simulations. Despite significant progress in reacting flows, mixture average diffusivities and neglect of Dufour effect are not uncommon. Turbulent reacting flows with complex chemistry are still at embryonic stages, with initial attempts in turbulent combustion using moderate size reaction mechanisms [116].

An example of a two-dimensional, non-isothermal fluid flow simulation is depicted in Fig. 7. This simulation indicates that the stagnation flow reactor used previously to extract kinetics can give rise to significant recirculations and contributions from the backside of the catalyst, indicating the inadequacy of the one-dimensional modeling analysis of experimental data. Due to the importance of transport phenomena and the potential contribution of gas-phase chemistry in partial oxidation and catalytic combustion, consideration to the coupling of CFD with gas and surface chemistries should be given. It is expected that extension to two- and three-dimensions will be materialized based on parallel, distributed computing platforms (e.g. Beowulf clusters).

4.1. Molecular-continuum coupling

To cope with the existence of multiple length and time scales involved in homogeneous–heterogeneous reactors depicted in Figs. 1 and 2, multiscale integration hybrid (MIH) algorithms are used. These algorithms are based on domain decomposition, where the fluid phase (macroscopic scales) is treated with continuum conservation equations, and the surface (mesoscopic scales) with a stochastic MC simulator.

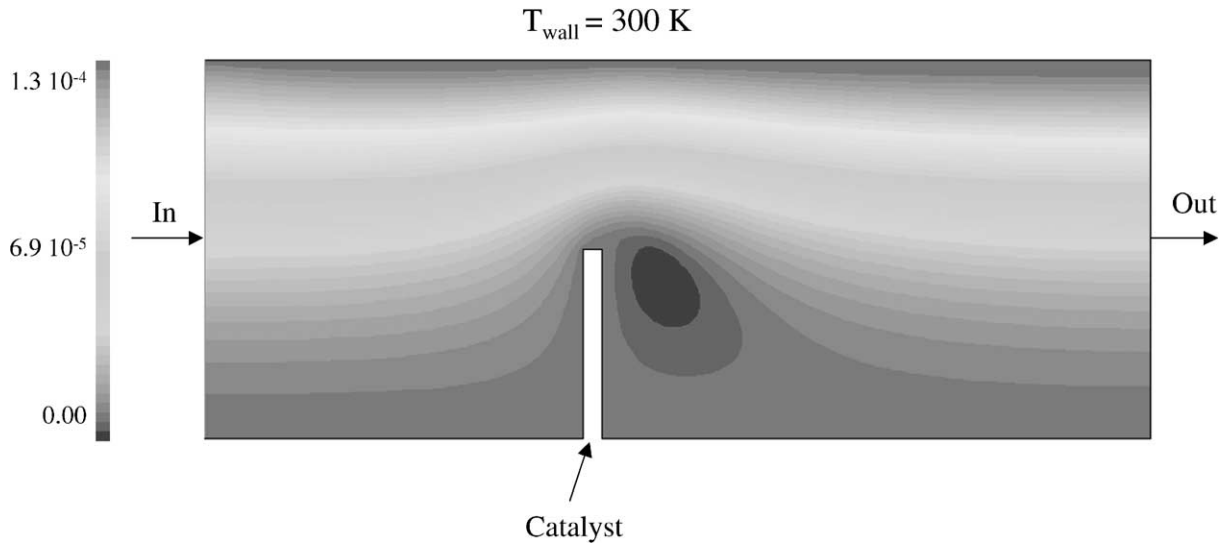

Fig. 7. Stream functions from a non-isothermal flow (air) simulation in a stagnation reactor enclosed in a glass tube. The catalyst is 1 mm thick × 20 mm wide and is maintained at 1000 K, whereas the rest of the boundaries are at 300 K. The inlet flow velocity is 0.5 m/s and the tube opening is 0.04 m wide. For certain conditions, flow recirculations occur explaining higher reactivity at the back of platinum foils seen in our lab. Chemical isolation of the back of the surface and proper description of transport are necessary for extraction of kinetics from this reactor.

Two numerical schemes are considered in solving such multiscale systems. First, a direct numerical simulation (DNS), which dynamically couples the gas-phase equations of change with the atomistic scale, is attempted. The gas-phase is solved using either an explicit Euler method (for simplicity) or the LSODA package, whereas the surface is modeled using the efficient continuous time MC with local update algorithm [69]. The spatially averaged surface rates from the MC simulation are provided to the gas-phase equations, which in turn provide the updated gaseous mole fractions needed in MC. The first demonstration of feasibility of such MIH algorithm was done several years ago for a prototype unimolecular surface reaction in a CSTR [63]. Subsequently, boundary value problems have been also addressed [117,118].

The feasibility of the DNS approach for detailed surface kinetics is illustrated for the first time in Fig. 8 with the example of catalytic CO oxidation on a platinum surface embedded in a CSTR. Fig. 8 shows the mole fractions (a) and the surface coverages (b) as a function of time. At very short times, changes in the surface coverages occur while the gas-phase is not practically changing (it serves as a buffer in this case or species in excess). At longer times (a small fraction of residence time), a strong coupling between the surface coverages and the gas-phase mole fractions is seen. Finally, at longer times (order of residence time), the system evolves with the slow dynamics of the gas-phase and eventually reaches steady state. DNS simulations are efficient when the catalytic system exhibits fast dynamics and strong coupling, whereas they can become computationally very demanding around turning points where slow dynamics is observed [119].

Numerical difficulties are sometimes encountered in these DNS MIH simulations due to the MC noise, which propagates into the fluid phase. This noise can make the entire numerical scheme unstable when rare event dynamics are encountered, where the rates change dramatically over a single event. Furthermore, while the time step, determined from the MC simulator, is typically very small, this is not always the case. For example, when an almost O* poisoned surface is simulated (slow desorption), the MC time step can become huge, rendering unstable the gas-phase integrator. In this case, one can advance the gas-phase with normal time steps till the MC time step is reached.

Following ideas proposed in [117], an iterative, splitting scheme can be also employed that involves iterative convergence of both the MC simulator and the gas-phase. Practically, the two scales are solved independently in every iteration, and the quantities coupling both models are computed. In particular, steady state surface rates computed from a MC simulator are incorporated into the steady state gas-phase conservation equations, which in turn provide the gas-phase mole fractions needed in the MC simulator (in the adsorption steps). This iterative scheme is computationally less demanding and allows parametric studies, i.e. an extension of natural parameter continuation algorithm from continuum to multiscale simulations. It obviously lacks transient information but it is convenient for steady state solutions. Fig. 9 shows the changes in reaction rate when the surface temperature is progressively increased around the

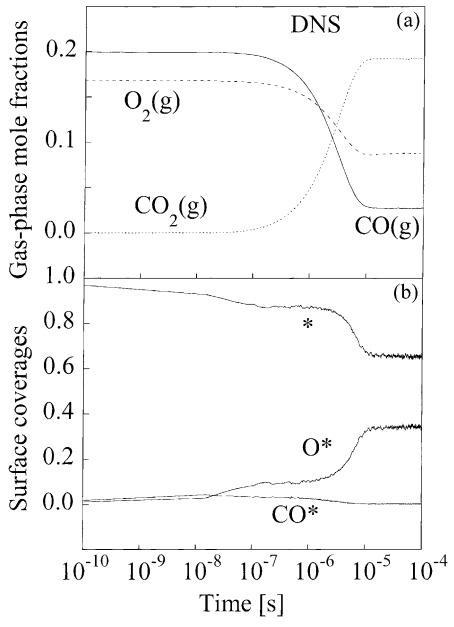

Fig. 8. Gas-phase mole fractions (a) and surface coverages (b) vs. real time for 20% CO in air in a CSTR operating at atmospheric pressure, at a surface temperature of 1200 K, and a contact time of 10^{-5} s. These simulations were conducted using the DNS algorithm, illustrating the feasibility of MIH algorithms and the strong coupling between the gas-phase and the catalytic surface. No lateral interactions were included in these simulations.

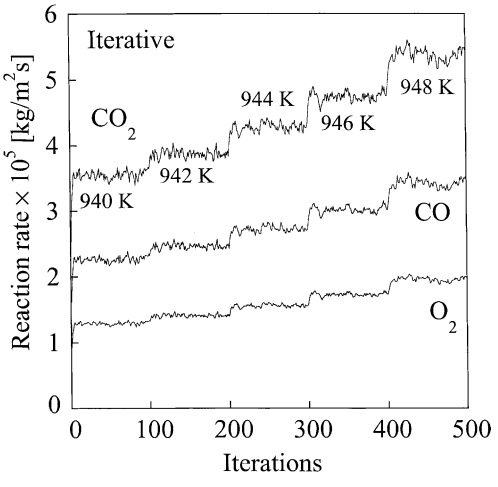

Fig. 9. Illustration of convergence of multiscale simulations using an iterative solver. The net reaction rates of the three gaseous species vs. iterations are depicted for increments in temperature near but prior to ignition. Visual inspection of rates indicates that they obey overall reaction stoichiometry. The number of iterations per temperature is much larger than what typically needed in the simulations for figure clarity. The parameters are the same as in Fig. 8.

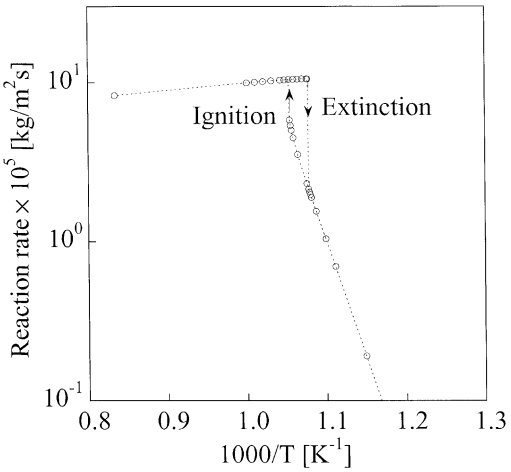

Fig. 10. Reaction rate vs. inverse temperature for the conditions of Fig. 8. The MIH algorithm illustrates complex dynamic behavior, including hysteresis, observed in catalytic systems.

ignition temperature versus the number of iterations. Every iteration entails the solution of gas-phase equations at steady state along with MC integration till steady state has been reached. For the MC simulator, automatic criteria have been implemented to guarantee steady state and obtain spatial average, steady state rates needed in the gas-phase simulator.

Fig. 10 shows the steady state reaction rate versus the inverse temperature, demonstrating the feasibility of such MIH algorithms for complex surface kinetics. Furthermore, non-linear phenomena, such as ignition and extinction, can be captured. From our experience, at low temperatures and near turning points, the iterative scheme is preferred because the coupling is weak and the dynamics is very slow. However, at higher temperatures, where the coupling becomes significant and the dynamics is fast, lack of convergence of the iterative scheme may be encountered [90], and thus, the DNS method is preferred.

5. Parameter optimization of molecular and multiscale simulators

Refined kinetic parameters used in a reaction mechanism are needed to accurately capture a wide variety of experimental features, ranging from spectroscopic data to reactor design responses. A multistep methodology was recently proposed and successfully applied to optimize the pre-factors of MF simulators [44,45]. We show here for the first time that this methodology can naturally be extended to molecular and multiscale models as well. This is illustrated for the oxidation of CO including the steps listed in Table 1 with surface diffusion, using the MC algorithm detailed elsewhere [69].

The first-step of the methodology is to estimate initial kinetic parameters for all the reaction steps involved in a screening reaction mechanism of the surface simulator according to the discussion above. The optimization methodology is then applied to refine the pre-factors (sticking coefficients and pre-exponentials) of the different steps. Using this screening mechanism, the important pre-factors affecting the experimental features under study are determined through SA. An important advantage of this multistep procedure is that it enables us to simultaneously analyze considerably different experimental data, ranging from vacuum to high pressure, from single crystals to practical catalysts, and from spectroscopic data to engineering responses of conversion, selectivity, ignition, and extinction. SA allows us to create a mapping between key mechanistic aspects of a large reaction mechanism and different experiments. Consequently, suitable experiments can be proposed. As an example, the oxygen-assisted path of methane decomposition on platinum predicted by simulations (and discussed in Fig. 4) was qualitatively verified in transient experiments in our lab [25]. The ultimate outcome of the approach is that refined reaction mechanisms are reliable over a wide range of experimental conditions.

As a simple example, in the catalytic oxidation of CO on platinum at 500 K, the adsorption–desorption of CO and the adsorption of O_2 are important steps in controlling the reaction rate for fuel rich mixtures. Furthermore, near the surface stoichiometric point where the reaction rate is maximum, surface diffusion needs to be included in the model optimization. SA determines then the target sets of experiments and suitable operating conditions to conduct the optimization. Details are given in [80].

A direct optimization using a molecular or multiscale model cannot be practically achieved because it requires a huge number of function evaluations, i.e. molecular or multiscale simulations. To circumvent this difficulty, a solution mapping technique is employed where the model response, e.g. reaction rate, ignition temperature, etc. is parameterized using low degree polynomials [120]. Simulated annealing is finally used to get the optimized pre-factors [121] (other choices are possible too). Finally, the parameters are validated against experiments not used in the optimization process.

Fig. 11 shows an example of performance of an optimized parameter model using our MC simulator for the reaction rate versus the CO:O_2 ratio data at 500 K. This multistep methodology yields satisfactory results for molecular models including surface diffusion at conditions where optimization was not performed (e.g. 400 and 600 K shown also in the same plot). Furthermore, due to its modularity, it can be easily applied to different types of experiments to provide a mechanism that is accurate over a wide range of conditions. It has also been shown [80], that for the same target experiments, some of the refined parameters of the surface mechanism derived from molecular models differ statistically from the ones derived from a continuum approach, justifying the need for extending these optimization tools to molecular and multiscale models. We propose that this approach could be used to fit complex force fields to quantum

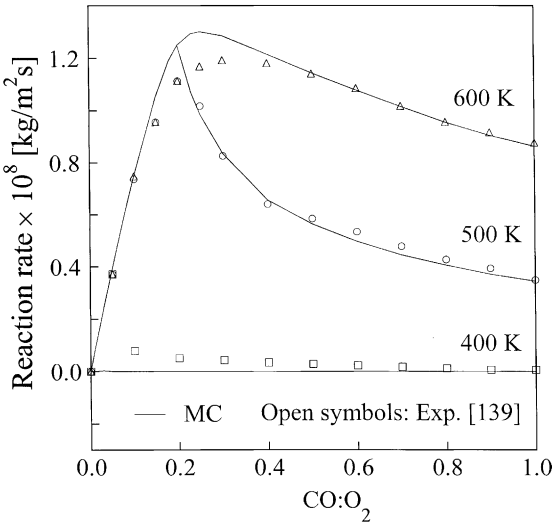

Fig. 11. Reaction rate vs. the $CO:O_2$ ratio comparing the optimized MC model (lines) against experimental data (symbols) of Liu et al. [139] at three temperatures. The parameters are refined at 500 K against the experiments carried out under ultra high vacuum conditions on a Pt(1 1 1) surface with a fixed molar total flux of 1.65×10^{18} molecules/(m^2 s). Lateral CO^*–CO^* interactions were considered in the CO desorption step only.

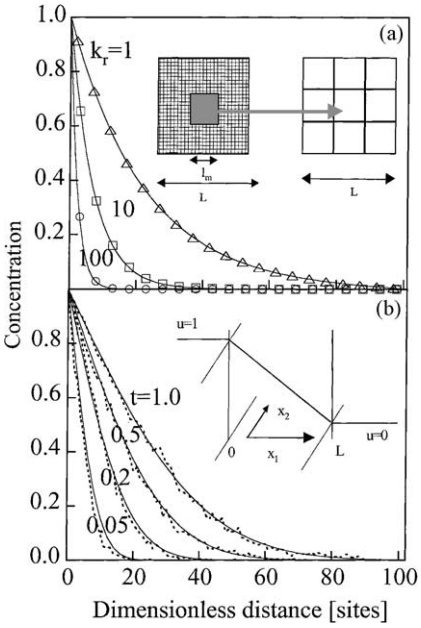

Fig. 12. Validation of gradient continuous time MC (G-CTMC) simulations in two-dimensions with continuum equation. (a) Steady state concentration profiles from Fickian diffusion with first-order surface reaction for three reaction rate constants indicated and (b) transient concentration profiles from Fickian diffusion at dimensionless times indicated (no other processes included). In both cases, Dirichlet boundary conditions of one and zero are used in the direction of diffusion and periodic boundary conditions are employed in the transverse direction. No interactions between atoms are considered. The insets in panels a and b depict the coarse-graining idea and simulation domain, respectively.

mechanical simulations, e.g. in zeolite materials, in order to eliminate the commonly used trial-and-error approach.

6. A mesoscopic framework for surface processes

In the presence of microscopic size inhomogeneities (of the order of a few nanometers), such as the ones shown in Fig. 1b, spatial averaging in a relatively large MC cell is sufficient to provide mesoscopically average rates needed in the fluid phase. However, experiments and continuum diffusion-reaction simulations clearly demonstrate that large scale patterns with characteristic wavelength of the order of micron(s) can form as a result of competition of diffusion and reaction processes (e.g. a Turing type instability) or microphase separation and reaction [122,123]. Local stability analysis indicates that the existence and wavelength of these patterns strongly depends on the actual value of species diffusivities [123,124]. Therefore, such mesoscale problems cannot be handled either by the asymptotic approach proposed above or other proposed assumptions found in the literature.

The recent introduction of mesoscopic equations for diffusion, as well as additional processes (e.g. molecular adsorption, desorption, and first-order surface reaction), provides an alternative, systematic framework to meet this challenge [6,125–132]. These are stochastic integrodifferential equations (SPDEs) derived directly from the underlying master equation (see Eq. (4)) solved conventionally, at small scales though, with MC methods. Their derivation entails coarse-graining using non-equilibrium statistical mechanics techniques over a relatively large area containing enough molecules or atoms (see schematic in Fig. 12) so that the local coverage can be replaced with a continuum rather than a discrete variable [130]. In contrast to ad hoc coarse-graining modeling, it can be shown that the derived mesoscopic equations are exact in the limit of an infinite range potential of interactions between species. While this appears to be restrictive, as interactions are short-ranged in many catalytic reaction applications, computations indicate that they are quantitative accurate for relatively short-range interactions [6,130]. It turns out that this is not a coincidence but a result of underlying properties. In particular, these equations obey a Large Deviation Principle and approach the infinite potential range behavior in an exponential fast manner as the potential length or the coordination of the lattice increases [131].

An important feature of mesoscopic equations is that coarse-graining retains the information of microscopic dynamics of diffusion in the rescaled equation. As a result, mesoscopic equations differ for various diffusion mechanisms (e.g. Metropolis versus Arrhenius). As an example, in the case of a unimolecular reaction

$$A+^* \leftrightarrow A^*$$

$$A^* \rightarrow B+^*$$

where intermolecular forces in desorption and diffusion are important, the mesoscopic equation under isothermal conditions (by leaving the noise terms out) reads

$$\frac{\partial u}{\partial t} - D\nabla\left\{e^{-\beta K^* u}\left[\nabla u - \beta u(1-u)\nabla K^* u\right]\right\} - k_a P(1-u) + k_d u e^{-\beta K^* u} + k_r u = 0 \quad (5)$$

Here t is the time, u the coverage (dimensionless concentration), $D = de^{-\beta U_0}$is the diffusion coefficient, d the diffusion coefficient at high (infinite) temperature, U_0 the energy associated with the binding of the catalyst, K the intermolecular potential of adsorbate–adsorbate (lateral) interactions, $K^*u = \int K(|r-r'|)u(r')dr'$is the convolution of the potential of interactions K and concentration u, k_a, k_d, and k_r are the rate constants for adsorption, desorption, and reaction, respectively, P is the reactant partial pressure, and $\beta^{-1} = kT$, with k being the Boltzmann constant and T being the temperature. In deriving Eq. (5), Arrhenius migration dynamics, i.e. the activation energy of jumping of species A depends on its binding energy only, and equal potential of interactions for desorption and migration have been assumed (see [132] for a more general case).

In the absence of lateral interactions and when the adsorption–desorption reaction terms are negligible, Eq. (5) reduces to Fick's second law of diffusion. It is interesting to notice that the diffusion in Eq. (5) is comprised of the normal Fickian term ($D\nabla^2 u$) and a correction term taking into account adsorbate–adsorbate interactions. In particular, the term $u(1-u)$ indicates the probability of migration from one occupied site to an adjacent empty site and the convolution term indicates the energy due to adsorbate–adsorbate interactions. The remaining last three terms represent the unimolecular reaction rates for adsorption, desorption, and reaction. Note that in these mesoscopic models, interactions enter the transport equation in a different way than in previous work [133–135]. Furthermore, Eq. (5) can also predict uphill diffusion under certain conditions [130]. The diffusion in Eq. (5) can also be cast in a more traditional form as a gradient in chemical potential [6]. The apparently complicated form of diffusion is due to a more complex form of the free energy functional in the presence of adsorbate–adsorbate interactions.

In order to test the accuracy of mesoscopic equations, we have recently proposed to force the system far away from equilibrium [6], so that non-zero fluxes and rates can be computed, and subsequently, to compare MC simulations to mesoscopic calculations for relatively short scale systems where the former are feasible. Figs. 12 and 13 compare solutions of the mesoscopic equation to gradient continuous time MC (G-CTMC) results under an overall gradient in concentration, i.e. a situation far from equilibrium. Physically, this situation arises in membrane reactors and microporous catalyst particles (e.g. zeolites), when the active sites are within the membrane or the particle, and in tubular type of reactor, where gradients are introduced by the gas-phase due to consumption of reactants.

First in Fig. 12, two examples are shown where comparison of the continuum solution with gradient MC simulations is carried out for non-interacting systems in two-dimensions, as a validation means of the latter. Note that the continuum equation is correct in this case, except of a higher order correction term that is neglected in passing to the continuum limit. Excellent agreement is seen in Fig. 12a even when the reaction is fast (in dimensionless units), that results in a thin boundary layer within the system. Similar agreement is obtained for transient situations as well, as indicated by an example in Fig. 12b in dimensionless time units. The overall agreement indicates the validity of our gradient MC simulation as well as the accuracy of continuum equations in the absence of intermolecular forces down to small scales and for relatively large gradients.

Next we present an example when intermolecular forces are important. Fig. 13 depicts steady state concentration profiles for one-dimensional and two-dimensional simulations for a piecewise constant potential extending over various possible number of neighbors in two-dimensions (for details see [130]). The one-dimensional simulations are done with the same total number of neighbors in each case as the two-dimensional simulations, and thus a longer potential than in the two-dimensional. It is found that repulsive interactions between species considerably increase

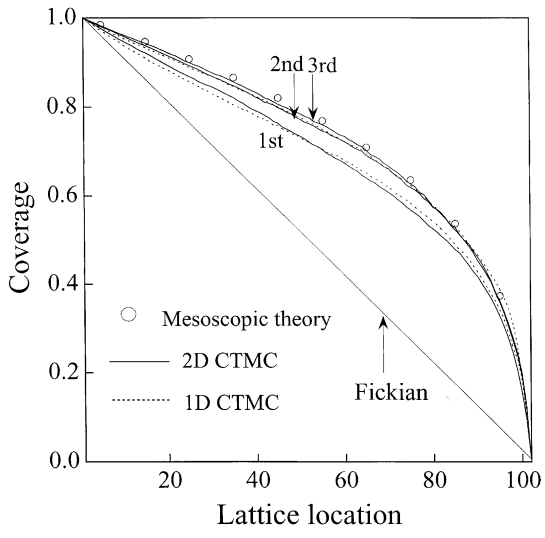

Fig. 13. Validation of the mesoscopic Eq. (5) (circles) with gradient continuous time MC (G-CTMC) simulations in one- (dotted lines) and two-dimensions (solid lines) for a piecewise constant potential of repulsive interactions (dimensionless potential strength of $\beta w = 1$). The straight line corresponds to a Fickian case. The numbers displayed indicate the number of neighbors included in the two-dimensional simulations. For the one-dimensional simulations, the same total number of neighbors has been used as in the two-dimensional simulations (e.g. four for the first nearest neighbor case corresponding to a square lattice) by appropriately adjusting the potential length. The boundary conditions are the same as in Fig. 12.

the diffusion flux over the Fickian case (a straight line depicted in Fig. 13). As the dimensionality of cubic lattices or the coordination of the lattice increases, shorter-range interactions are needed to achieve quantitative agreement between the mesoscopic and MC simulations. It is expected that for practical systems, the mesoscopic framework will be sufficiently accurate. As a final point, for sufficiently strong and long interactions, complex patterns and even uphill diffusion can be seen for different potentials, which is beyond any classic continuum diffusion-reaction model of a single species [130]. Note that the Stefan–Maxwell equations can also predict uphill diffusion for binary non-interacting mixtures but they cannot treat, in a fundamental way, intermolecular forces [136]. Furthermore, while continuum Cahn–Hilliard-type equations can predict uphill diffusion for a single interacting species [137], there are still used in a phenomenological manner, limited to attractive interactions only, and neglect higher order gradient corrections.

The continuum nature of mesoscopic equations enables one to apply homogenization techniques in order to study spatially heterogeneous materials. An interesting application encompasses faceted catalysts encountered in partial oxidation reactions (e.g. gauzes) and supported catalyst particles. In both cases, coupling between various patches (facets or support and catalyst particles) of the system is important. Such an approach can replace current intensive MC simulations [72]. We have recently developed such homogenized mesoscopic equations and validated them through DNS [138]. For example, homogenization of the above mesoscopic equation gives

$$\frac{\partial u_0}{\partial t}\Omega = \sum_k \frac{\partial}{\partial x_k}\left[\sum_i D_{k_i}^{\mathrm{eff}} u_0(1-u_0)\frac{\partial}{\partial x_i} \times \left(\ln\left[\frac{u_0}{(1-u_0)}\right] - \beta a_0 K^* b_0 u_0\right)\right] + k_r^{\mathrm{eff}} u_0 \quad (6)$$

where $k_{\mathrm{r}}^{\mathrm{eff}} = \frac{1}{\Omega}\int_Y k_{\mathrm{r}}\mathrm{d}Y$, $a_0 = \frac{1}{\Omega}\int_Y a(y)\mathrm{d}y$, $b_0 = \frac{1}{\Omega}\int_Y b(y)\,\mathrm{d}y$, $\Omega = \int_Y \mathrm{d}y$, $a_0 J^* b_0 u_0 = a_0 b_0 \int_{-\infty}^{+\infty} K(|x-r|)u_0(r)\mathrm{d}r$ with $D_{k_i}^{\mathrm{eff}} = \int_Y \left(D\left(\delta_{ik} + \frac{\partial \chi_i}{\partial y_k}\right)\right)\mathrm{d}y$ for Metropolis dynamics and $D_{k_i}^{\mathrm{eff}} = \mathrm{e}^{-a_0 K^* b_0 u_0}\int_Y \left(D\left(\delta_{ik} + \frac{\partial \chi_i}{\partial y_k}\right)\right)\mathrm{d}y$ for Arrhenius dynamics. Here δ is the Kronecker function and χ the solution of:

$$\sum_k \sum_l \left[\frac{\partial}{\partial y_l}\left(D\frac{\partial \chi_i}{\partial y_k}\right)\right] = -\sum_l \frac{\partial D}{\partial y_l} \quad (7)$$

All the summations, here, extend over the dimensionality of the problem. Furthermore, a_0 and b_0 are the leading order terms of a and b, which indicate the type of medium, u_0 is the leading order term of the solution u, and W is the domain. Details of the derivation, numerical procedures, and examples, for diffusion as the only mechanism, are given elsewhere [130].

Currently, mesoscopic equations have been derived for a single species and for simple adsorption, desorption, and surface reaction mechanisms. It would be then desirable to extend them from model systems to more complex situations of practical interest and compare simulation results to experimental data. Furthermore, coupling of mesoscopic models with continuum models is highly desirable.

7. Summary and outlook

We have described a multiscale, hierarchical computational framework for modeling chemical reactors, to describe phenomena that occur over multiple length and time scales and are strongly coupled. We have focused mainly on catalytic systems, and specifically on the oxidation of CO and CH_4 on noble metals, as specific examples for illustration. The computational feasibility of such multiscale simulations linking scales from the quantum, to the molecular, to the mesoscopic, to the continuum has been demonstrated. An efficient methodology for parameter optimization has been also discussed. Finally, homogenization of mesoscopic equations has been introduced that enables one to predict spatially average properties of polycrystalline catalysts while retaining molecular and quantum level information. This approach along with further developments in mesoscopic models will pave the way in linking all scales. Pattern formation on catalytic surfaces and first principle simulations of processes in membranes and catalyst particles are just examples where this mesoscopic modeling is expected to have direct impact.

There is a continuous need for more accurate and predictive models with input from first principles. Therefore, one may expect intensification of research efforts on multiscale modeling. Multiscale algorithms remain though computationally demanding. Thus, modern model reduction techniques (e.g. computational singular perturbation, low-dimensional manifold theory, etc.) employed for transport and gas-phase chemistry problems can be easily extended to these multiscale systems to enable on line control and practical reactor design. One example of multiscale model reduction has just appeared [15], but more are expected in the future. Furthermore, robustness and efficiency of solution of multiscale problems are expected to grow in the future.

Acknowledgements

Acknowledgement for partial support of this work is made to the National Science Foundation (CAREER Award no. CTS-9702615). Stimulating discussions with Profs. M. Tsapatsis and M. Katsoulakis are also acknowledged. Insightful comments on zeolite modeling by Prof. S.M. Auerbach are appreciated. We also thank D. Norton for performing fluent simulations depicted in Fig. 7,

and T. Basak and R. Lam for results shown in Figs. 12 and 13.

References

[1] M. Bodenstein, Z. Physik Chem. 85 (1913) 329.
[2] W.M. Deen, Analysis of Transport Phenomena, Oxford University Press, New York, 1998.
[3] F.A. Williams, Combustion theory: The Fundamental Theory of Chemically Reacting Flow Systems, Benjamin/Cummings, Menlo Park, CA, 1985.
[4] K.E. Brenan, S.L. Campbell, L.R. Petzold, Numerical Solution of Initial-Value Problems in Differential-Algebraic Equations, SIAM, Philadelphia, 1996.
[5] C.W. Gear, Numerical Initial-Value Problems in Ordinary Differential Equations, Prentice-Hall, Englewood Cliffs, NJ, 1971.
[6] D.G. Vlachos, M.A. Katsoulakis, Derivation and validation of mesoscopic theories for diffusion of interacting molecules, Phys. Rev. Lett. 85 (18) (2000) 3898.
[7] J.J. Lerou, K.M. Ng, Chemical reaction engineering: a multiscale approach to a multiobjective task, Chem. Eng. Sci. 51 (10) (1996) 1595.
[8] J. Villermaux, New horizons in chemical engineering, in: Proceedings of the Plenary Lecture in Fifth World Congress of Chemical Engineering, San Diego, CA, 15 July 1996.
[9] T.B. Thompson, Chemical industry of the future: technology roadmap for computational chemistry, DOE Workshop Roadmap for Computational Chemistry, 1999 (http://itri.loyola.edu/molmodel).
[10] N.G. Hadjiconstantinou, A.T. Patera, Heterogeneous atomistic continuum representations for dense fluid systems, Int. J. Mod. Phys. C 8 (4) (1997) 967.
[11] S.T. O'Connell, P.A. Thompson, Molecular dynamics-continuum hybrid computations: a tool for studying complex fluid-flows, Phys. Rev. E 52 (6) (1995) 5792.
[12] S.T. Rodgers, K.F. Jensen, Multiscale modeling of chemical vapor deposition, J. Appl. Phys. 83 (1) (1998) 524.
[13] K.F. Jensen, S.T. Rodgers, R. Venkataramani, Multiscale modeling of thin film growth, Curr. Opin. Solid State Mater. Sci. 3 (6) (1998) 562.
[14] R. Lam, D.G. Vlachos, A multiscale model for epitaxial growth of films: growth mode transition, Phys. Rev. B 64 (3) (2001) 035401.
[15] S. Raimondeau, D.G. Vlachos, Low-dimensional approximations of multiscale epitaxial growth models for microstructure control of materials, J. Comp. Phys. 160 (2000) 564.
[16] D. Maroudas, Multiscale modeling of hard materials: challenges and opportunities for chemical engineering, AIChE J. 46 (5) (2000) 878.
[17] J.J. Derby, P. Daoutidis, Y. Kwon, A. Pandy, P. Sonda, B. Vartak, A. Yeckel, M. Hainke, G. Muller, High-performance-computing. Multi-scale models for crystal growth systems, Mineapolis, MN, University of Minnesota, Supercomputing Institute Research Report UMSI 2001/50, 2001.
[18] A. Nakano, M. Bachlechner, R.K. Kalia, E. Lidorikis, P. Vashishta, G. Voyiadjis, T.J. Campbell, S. Ogata, F. Shimojo, Multiscale simulation of nanosystems, Comput. Sci. Eng. 3 (4) (2001) 56.
[19] U. Hansen, S. Rodgers, K.F. Jensen, Modeling of metal thin film growth: linking angstrom-scale molecular dynamics results to micron-scale film topographies, Phys. Rev. B 62 (4) (2000) 2869.
[20] T.P. Merchant, M.K. Gobbert, T.S. Cale, L.J. Borucki, Multiple scale integrated modeling of deposition processes, Thin Solid Films 365 (2000) 368.
[21] D.O. Drews, Multiscale simulations of copper electrodeposition from a multiple additive system, M.S. thesis, Department of Chemical Engineering, University of Illinois, Urbana-Champaign, 2001.
[22] D.A. Hickman, E.A. Haupfear, L.D. Schmidt, Synthesis gas-formation by direct oxidation of methane over Rh monoliths, Cat. Lett. 17 (3-4) (1993) 223.
[23] L.D. Pfefferle, W.C. Pfefferle, Catalysis in combustion, Catal. Rev. Sci. Eng. 29 (1987) 219.
[24] C.N. Satterfield, Heterogeneous Catalysis in Industrial Practice, 2nd Edition, McGraw-Hill, New York, 1991.
[25] P. Aghalayam, Y.K. Park, D.G. Vlachos, Partial oxidation of light alkanes in short contact time microreactors, Catalysis 15 (2000) 98.
[26] D.A. Goetsch, L.D. Schmidt, Microsecond catalytic partial oxidation of alkanes, Science 271 (1996) 1560.
[27] R.J. Kee, F.M. Rupley, J.A. Miller, CHEMKIN-II: a FORTRAN chemical kinetics package for the analysis of gas-phase chemical kinetics, Livermore, CA, Sandia National Laboratories Report, SAND89-8009, 1991.
[28] R.J. Kee, F.M. Rupley, J.A. Miller, The CHEMKIN thermodynamic data base, Sandia National Laboratories Report, SAND87-8215B, 1991.
[29] R.J. Kee, G. Dixon-Lewis, J. Warnatz, M.E. Coltrin, J.A. Miller, A FORTRAN computer code package for the evaluation of gas-phase multicomponent transport properties, Sandia National Laboratories Report, SAND86-8246, 1990.
[30] G.P. Smith, D.M. Golden, M. Frenklach, N.W. Moriarty, B. Eiteneer, M. Goldenberg, C.T. Bowman, R.K. Hanson, S. Song, W.C.J. Gardiner, V.V. Lissianski, Z. Qin, GRI-mech 3.0: Gas-Research-Institute mechanism for natural gas, taken from http://www.me.berkeley.edu/gri_mech/, 2000.
[31] I.A. Dumesic, D.F. Rud, L.M. Aparicio, J.E. Rekoske, A.A. Revino, The Microkinetics of Heterogeneous Catalysis, American Chemical Society, Washington, DC, 1993.
[32] C.K. Westbrook, F.L. Dryer, Chemical kinetics and modeling of combustion processes, in: Proceedings of the Eighteenth International Symposium on Combustion, The Combustion Institute, Pittsburgh, 1981.
[33] P.J. Clymans, G.F. Froment, Computer-generation of reaction paths and rate-equations in the thermal-cracking of normal and branched paraffins, Comput. Chem. Eng. 8 (2) (1984) 137.
[34] C. Chevalier, W.J. Pitz, J. Warnatz, C.K. Westbrook, H. Melenk, Hydrocarbon ignition: automatic generation of reaction mechanisms and applications to modeling of engine knock, in: Proceedings of the International Symposium on Combustion, The Combustion Institute, Pittsburgh, Vol. 24, 1992, p. 93.
[35] M. Dente, S. Pierucci, E. Ranzi, New improvements in modeling kinetic schemes for hydrocarbons pyrolysis reactors, Chem. Eng. Sci. 47 (9–11) (1992) 2629.
[36] L. Broadbelt, S.M. Stark, M.T. Klein, Computer-generated pyrolysis modeling-on-the-fly generation of species, reactions, and rates, Ind. Eng. Chem. Res. 33 (4) (1994) 790.
[37] R.G. Susnow, A.M. Dean, W.H. Green, P. Peczak, L. Broadbelt, Rate-based construction of kinetic models for complex systems, J. Phys. Chem. A 101 (1997) 3731.
[38] A.V. Zeigarnik, R.E. Valdes-Perez, B.S. White, Proposed methodological improvement in the elucidation of chemical reaction mechanisms based on chemist-computed interaction, J. Chem. Edu. 77 (2) (2000) 214.
[39] Y.K. Park, P. Aghalayam, D.G. Vlachos, A generalized approach for predicting coverage-dependent reaction parameters of complex surface reactions: application to H_2 oxidation over platinum, J. Phys. Chem. A 103 (40) (1999) 8101.
[40] D.G. Vlachos, L.D. Schmidt, R. Aris, Ignition and extinction of flames near surfaces: combustion of CH_4 in air, AIChE J. 40 (6) (1994) 1005.
[41] P.-A. Bui, D.G. Vlachos, P.R. Westmoreland, Catalytic ignition of methane/oxygen mixtures over platinum surfaces: comparison of detailed simulations and experiments, Surf. Sci. 385 (2/3) (1997) L1029.

[42] O. Deutschmann, F. Behrendt, J. Warnatz, Modeling and simulation of heterogeneous oxidation of methane on a platinum foil, Catal. Today 21 (1994) 461.
[43] D.A. Hickman, L.D. Schmidt, Steps in CH_4 oxidation on Pt and Rh surfaces: high temperature reactor simulations, AIChE J. 39 (7) (1993) 1164.
[44] P. Aghalayam, Y.K. Park, D.G. Vlachos, Construction and optimization of detailed surface reaction mechanisms, AIChE J. 46 (10) (2000) 2017.
[45] P. Aghalayam, Y.K. Park, D.G. Vlachos, A detailed surface reaction mechanism for CO oxidation on Pt, in: Proceedings of the International Symposium on Combustion, Edinburgh, Scotland, Vol. 28, 2000, p. 1331.
[46] M.J. De Witt, D.J. Dooling, L. Broadbelt, Computer generation of reaction mechanisms using quantitative rate information: application to long-chain hydrocarbon, Ind. Eng. Chem. Res. 39 (2000) 2228.
[47] G.F. Froment, Kinetic modeling of complex catalytic reactions, Rev. Inst. Petrole 46 (4) (1991) 491.
[48] W. Feng, E. Vynckier, G.F. Froment, Single-event kinetics of catalytic cracking, Ind. Eng. Chem. Res. 33 (12) (1993) 2997.
[49] M. Witko, Oxidation of hydrocarbons on transition-metal oxide catalysts: quantum chemical studies, J. Mol. Cat. 70 (3) (1991) 277.
[50] F. Ruette, Quantum Chemistry Approaches to Chemisorption and Heterogeneous Catalysis, Kluwer Academic Publishers, Dordrecht, 1992.
[51] R.A. van Santen, M. Neurock, Concepts in theoretical heterogeneous catalytic reactivity, Catal. Rev. Sci. Eng. 37 (1995) 557.
[52] E. Shustorovich, Chemisorption phenomenon: analytic modeling based on perturbation theory and bond-order conservation, Surf. Sci. Rep. 6 (1986) 1.
[53] E. Shustorovich, H. Sellers, The UBI-QEP method: a practical theoretical approach to understanding chemistry on transition metal surfaces, Surf. Sci. Rep. 31 (1998) 1.
[54] P. Aghalayam, Y.K. Park, N.E. Fernandes, D.G. Vlachos, A C1 mechanism for methane oxidation on platinum, J. Catal., (2002) submitted.
[55] G. Ertl, Reactions at well-defined surfaces, Surf. Sci. 299/300 (1994) 742.
[56] R. Masel, Principles of Adsorption and Reaction on Solid Surfaces, in Principles of Adsorption and Reaction on Solid Surfaces. Part I, Wiley, New York, 1996, p. 284.
[57] N. Metropolis, A.W. Rosenbluth, M.N. Rosenbluth, A.H. Teller, E. Teller, Equation of state calculations by fast computing machines, J. Chem. Phys. 21 (1953) 1087.
[58] K. Binder (Ed.), Monte Carlo methods in Statistical Physics, Vol. 7, Springer, Berlin, 1986.
[59] M.P. Allen, D.J. Tildesley, Computer Simulation of Liquids, Oxford Science Publications, Oxford, 1989.
[60] E. Wicke, P. Kunmann, W. Keil, J. Schiefler, Unstable and oscillatory behavior in heterogeneous catalysis, Berichte der Bunsen-Gesellschaft-Phys. Chem. Chem. Phys. 84 (4) (1980) 315.
[61] R.M. Ziff, E. Gulari, Y. Barshad, Kinetic phase transitions in an irreversible surface-reaction model, Phys. Rev. Lett. 56 (24) (1986) 2553.
[62] R. Nieminen, A. Jansen, Monte Carlo simulations of surface reactions, Appl. Catal. A: Gen. 160 (1997) 99.
[63] D.G. Vlachos, L.D. Schmidt, R. Aris, The effects of phase transitions, surface diffusion, and defects on surface catalyzed reactions: oscillations and fluctuations, J. Chem. Phys. 93 (1990) 8306.
[64] D.G. Vlachos, L.D. Schmidt, R. Aris, The effect of phase transitions, surface diffusion, and defects on heterogeneous reactions: multiplicities and fluctuations, Surf. Sci. 249 (1991) 248.
[65] K.A. Fichthorn, W.H. Weinberg, Theoretical foundations of dynamical Monte Carlo simulations, J. Chem. Phys. 95 (2) (1991) 1090.
[66] A.P.J. Jansen, Monte Carlo simulations of chemical reactions on a surface with time-dependent reaction-rate constants, Comp. Phys. Commun. 86 (1995) 1.
[67] J. Lukkien, J. Segers, P. Hilbers, R. Gelten, A. Jansen, Efficient Monte Carlo methods for the simulation of catalytic surface reactions, Phys. Rev. E 58 (2) (1998) 2598.
[68] R. Kissel-Osterrieder, F. Behrendt, J. Warnatz, Detailed modeling of the oxidation of CO on platinum: a Monte Carlo model, in: Proceedings of the Twenty-Seventh International Symposium on Combustion, The Combustion Institute, 1998, p. 2267.
[69] J. Reese, S. Raimondeau, D.G. Vlachos, Monte Carlo algorithms for complex surface reaction mechanisms: efficiency and accuracy, J. Comp. Phys. 173 (1) (2001) 302.
[70] S.J. Lombardo, A.T. Bell, A review of theoretical models of adsorption, diffusion, desorption, and reaction of gases on metal-surfaces, Surf. Sci. Rep. 13 (1/2) (1991) 1.
[71] H. Chuan Kang, W.H. Weinberg, Modeling the kinetics of heterogeneous catalysis, Chem. Rev. 95 (1995) 667.
[72] V. Zhdanov, B. Kasemo, Simulations of the reaction kinetics on nanometer supported catalyst particles, Surf. Sci. Rep. 39 (2-4) (2000) 29.
[73] A. Jansen, J. Lukkien, Dynamic Monte Carlo simulations in heterogeneous catalysis, Catal. Today 53 (1999) 259.
[74] L. Broadbelt, R. Snurr, Applications of molecular modeling in heterogeneous catalysis research, Appl. Catal. A: Gen. 200 (2000) 23.
[75] V.P. Zhdanov, B. Kasemo, Kinetic phase transitions in simple reactions on solid surfaces, Surf. Sci. Rep. 20 (1994) 111.
[76] F. Qin, L. Tagliabue, L. Piovesan, E.E. Wolf, Monte Carlo simulations of self-sustianed oscillations of CO oxidation over non-isothermal supported catalysts, Chem. Eng. Sci. 53 (5) (1998) 919.
[77] M. Neurock, E.W. Hansen, First-principles-based molecular simulations of heterogeneous catalytic surface chemistry, Comput. Chem. Eng. 22 (1998) S1045.
[78] E.W. Hansen, M. Neurock, Modeling surface kinetics with first-principles-based molecular simulation, Chem. Eng. Sci. 54 (1999) 3411.
[79] S.J. Lombardo, A.T. Bell, A Monte Carlo model for the simulation of temperature-programmed desorption spectra, Surf. Sci. 206 (1998) 101.
[80] S. Raimondeau, P. Aghalayam, D.G. Vlachos, Parameter optimization in molecular models: Application to surface kinetics, Ind. Eng. Chem. Res., 2002, submitted.
[81] R. Gomer, Diffusion of adsorbates on metal surfaces, Rep. Prog. Phys. 53 (1990) 917.
[82] H. Brune, Microscopic view of epitaxial metal growth: nucleation and aggregation, Surf. Sci. Rep. 31 (1998) 121–229.
[83] R.H. Goodman, D.S. Graff, L.M. Sander, P. Leroux-Hugon, E. Clement, Trigger waves in a model for catalysis, Phys. Rev. E 52 (6) (1995) 5904.
[84] B. Meng, W.H. Weinberg, Non-equilibrium effects on thermal desorption spectra, Surf. Sci. 374 (1997) 443.
[85] J.L. Sales, R.O. Unac, V. Gargiulo, V. Bustos, G. Zgrablich, Monte Carlo simulation of temperature program desorption spectra: a guide through the forest for monomolecular adsorption on a square lattice, Langmuir 12 (1996) 95–100.
[86] M. Silverberg, A. Ben-Shaul, Adsorbate lateral interactions and islanding in surface reaction kinetics, Surf. Sci. 214 (1989) 17.
[87] M. Tammaro, M. Sabella, J.W. Evans, Hybrid treatment of spatio-temporal behavior in surface reactions with coexisting immobile and highly mobile reactants, J. Chem. Phys. 103 (23) (1995) 10277.
[88] H.C. Kang, W.H. Weinberg, Dynamic Monte Carlo with a proper energy barrier: surface diffusion and two-dimensional domain ordering, J. Chem. Phys. 90 (5) (1988) 2824.
[89] S.M. Auerbach, Theory and simulation of jump dynamics, diffusion and phase equilibrium in nanopores, Int. Rev. Phys. Chem. 19 (2) (2000) 155.

[90] S. Raimondeau, D.G. Vlachos, The role of adsorbate-layer non-uniformities in catalytic reactor design: Multiscale simulations for CO oxidation on Pt, Comput. Chem. Eng., 2002, in press.
[91] W.-S. Yang, H.-W. Xiang, Y.-W. Li, Y.-H. Sun, Microkinetic analysis and Monte Carlo simulation in methane partial oxidation into synthesis gas, Catal. Today 61 (2000) 237.
[92] S. Raimondeau, P. Aghalayam, D.G. Vlachos, M. Katsoulakis, Bridging the gap of multiple scales: from microscopic, to mesoscopic, to macroscopic models, in foundations of molecular modeling and simulation, Colorado, 2000, p. 155.
[93] S.J. Lombardo, A.T. Bell, Monte Carlo simulation of temperature-programmed desorption of co-adsorbed species, Surf. Sci. 224 (1989) 451.
[94] F.J. Keil, R. Krishna, M.O. Coppens, Modeling of diffusion in zeolites, Rev. Chem. Eng. 16 (2) (2000) 71.
[95] B.L. Trout, A.K. Chakraborty, A.T. Bell, Analysis of the thermochemistry of NO_x decomposition over Cu-ZSM-5 based on quantum chemical and statistical mechanical calculations, J. Phys. Chem. 100 (44) (1996) 17582.
[96] B.L. Trout, A.K. Chakraborty, A.T. Bell, Diffusion and reaction in ZSM-5 studied by dynamic Monte Carlo, Chem. Eng. Sci. 52 (14) (1997) 2265.
[97] M.J. Murphy, G.A. Voth, A.L.R. Bug, Classical and quantum transition state theory for the diffusion of helium in silica sodalite, J. Chem. Phys. B 101 (4) (1997) 491.
[98] T.N. Truong, Thermal rates of hydrogen exchange of methane with zeolite: a direct ab initio dynamics study on the importance of quantum tunneling effects, J. Chem. Phys. B 101 (15) (1997) 2750.
[99] Q.Y. Wang, S.R. Challa, D.S. Sholl, J.K. Johson, Quantum sieving in carbon nanotubes and zeolites, Phys. Rev. Lett. 82 (5) (1999) 956.
[100] J.T. Fermann, S.M. Auerbach, Modeling proton mobility in acidic zeolite clusters. Part II. Room temperature tunneling effects from semi-classical rate theory, J. Chem. Phys. 112 (15) (2000) 6787.
[101] J.T. Fermann, C. Blanco, S.M. Auerbach, Modeling proton mobility in acidic zeolite clusters. Part I. Convergence of transition state parameters from quantum chemistry, J. Chem. Phys. 112 (15) (2000) 6779.
[102] J. Sauer, M. Sierka, F. Haase, Transition state modeling for catalysis, in: D.G. Truhlar, K. Morokuma (Eds.), Transition State Modeling for Catalysis, American Chemical Society, Washington, 1999, p. 358.
[103] M. Sierka, J. Sauer, Finding transition structures in extended systems: a strategy based on a combined quantum mechanics-empirical valence bond approach, J. Chem. Phys. 112 (16) (2000) 6983.
[104] R. Hernandez, W.H. Miller, Semi-classical transition-state theory—a new perspective, Chem. Phys. Lett. 214 (2) (1993) 129.
[105] E.W. Hansen, M. Neurock, First-principles-based Monte Carlo simulation of ethylene hydrogenation kinetics on Pd, J. Catal. 196 (2000) 241.
[106] E.W. Hansen, M. Neurock, Predicting lateral surface interactions through density functional theory: application to oxygen on Rh(1 0 0), Surf. Sci. 441 (1999) 410.
[107] E.W. Hansen, M. Neurock, First-principles-based Monte Carlo methodology applied to O/Rh(1 0 0), Surf. Sci. 464 (2000) 91.
[108] S.J. Lombardo, A.T. Bell, Monte Carlo simulations of the effect of pressure on isothermal and temperature-programmed desorption kinetics, Surf. Sci. 245 (1991) 213.
[109] R.B. Bird, W.E. Stewart, E.N. Lightfoot, Transport Phenomena, Wiley, New York, 1960.
[110] P.A. Bui, D.G. Vlachos, P.R. Westmoreland, Modeling ignition of catalytic reactors with detailed surface kinetics and transport: combustion of H_2/air mixtures over platinum surfaces, Ind. Eng. Chem. Res. 36 (7) (1997) 2558.
[111] D.G. Vlachos, Two-dimensional detailed chemistry simulations in catalytic monoliths for methane combustion, in Eastern States Section, Hartford, CT, The Combustion Institute, Pittsburgh, 1997.
[112] U. Dogwiler, P. Benz, J. Mantzaras, Two-dimensional modeling for catalytically stabilized combustion of a lean methane-air mixture with elementary homogeneous and heterogeneous chemical reactions, Combust. Flame 116 (1/2) (1999) 243.
[113] O. Deutschmann, L.D. Schmidt, Modeling the partial oxidation of methane in a short-contact-time reactor, AIChE J. 44 (11) (1998) 2465.
[114] L.L. Raja, R.J. Kee, O. Deutschmann, J. Warnatz, L.D. Schmidt, A critical evaluation of Navier-Stokes, boundary-layer, and plug-flow models of the flow and chemistry in a catalytic-combustion monolith, Catal. Today 59 (1/2) (2000) 47.
[115] D.K. Zerkle, M.D. Allendorf, M. Wolf, O. Deutschmann, Modeling of on-line catalyst addition effects in a short contact time reactor, Proc. Comb. Inst. 28 (2000) 1365.
[116] J.Y. Chen, J.A. Blasco, N. Fueyo, C. Dopazo, S.B. Pope, A.R. Masari, An economical strategy for storage of chemical kinetics: fitting in situ adaptive tabulation with artificial networks, Proc. Comb. Inst. 28 (2000) 115.
[117] D.G. Vlachos, Multiscale integration hybrid algorithms for homogeneous–heterogeneous reactors, AIChE J. 43 (11) (1997) 3031.
[118] D.G. Vlachos, The role of macroscopic transport phenomena in film microstructure during epitaxial growth, Appl. Phys. Lett. 74 (19) (1999) 2797.
[119] S.K. Scott, Oscillations, waves, and chaos in chemical kinetics, in: R.G. Compton (Ed.), Oxford Chemistry Primers, Oxford Science Publications, Oxford, 1994.
[120] G.E.P. Box, N.R. Draper, Empirical Model-Building and Response Surfaces, Wiley, New York, 1987.
[121] S. Kirkpatrick, C.D. Gelatt Jr., M.P. Vecchi, Optimization by simulated annealing, Science 220 (4598) (1983) 671.
[122] A. Turing, The chemical basis of morphogenesis, Phil. Trans. R. Soc. London: Ser. B 237 (1952) 37.
[123] M. Hildebrand, A.S. Mikhailov, G. Ertl, Non-equilibrium stationary microstructure in surface chemical reactions, Phys. Rev. E 58 (2) (1998) 5483.
[124] J.D. Murray, Mathematical Biology, Springer, Heidelberg, 1989.
[125] J.L. Lebowitz, E. Orlandi, E. Presutti, A particle model for spinodal decomposition, J. Stat. Phys. 63 (5/6) (1991) 933.
[126] A. De Masi, E. Orlandi, E. Presutti, L. Triolo, I. Mesoscopic, Glauber evolution with KAC potentials. Part I. Mesoscopic and macroscopic limits, interface dynamics, Nonlinearity 7 (1994) 633.
[127] M. Hildebrand, A.S. Mikhailov, Mesoscopic modeling in the kinetic theory of adsorbates, J. Phys. Chem. 100 (1996) 19089.
[128] G. Giacomin, J.L. Lebowitz, Exact macroscopic description of phase segregation in model alloys with long range interactions, Phys. Rev. Lett. 76 (1996) 1094.
[129] M.A. Katsoulakis, P.E. Souganidis, Stochastic Ising models and anisotropic front propagation, J. Stat. Phys. 87 (1997) 63.
[130] R. Lam, T. Basak, D.G. Vlachos, M.A. Katsoulakis, Validation of mesoscopic theories and their application to computing effective diffusivities, J. Chem. Phys. 115 (24) (2001) 11278.
[131] M.A. Katsoulakis, D.G. Vlachos, Mesoscopic modeling of surface processes, in: Multiscale Models for Surface Evolution and Reacting Flows, Springer-Verlag, IMA, 2002, in press.
[132] M.A. Katsoulakis, D.G. Vlachos, From microscopic interactions to macroscopic laws of cluster evolution, Phys. Rev. Lett. 84 (7) (2000) 1511.
[133] S. Sundaresan, C.K. Hall, Mathematical modelling of diffusion and reaction in blocked zeolite catalysts, Chem. Eng. Sci. 41 (6) (1986) 1631.
[134] J.G. Tsikoyiannis, J. Wei, Diffusion and reaction in high-occupancy zeolite catalysts. Part I. A stochastic theory, Chem. Eng. Sci. 46 (1) (1991) 233.
[135] Y.D. Chen, R.T. Yang, Predicting binary Fickian diffusivities from pure-component Fickian diffusivities for surface diffusion, Chem. Eng. Sci. 47 (15/16) (1992) 3895.

[136] R. Krishna, J.A. Wesselingh, Review article no. 50: the Maxwell–Stefan approach to mass transfer, Chem. Eng. Sci. 52 (6) (1997) 861.
[137] J.W. Cahn, J.E. Hilliard, Free energy of a non-uniform system. Part I. Interfacial free energy, J. Chem. Phys. 28 (1958) 258.
[138] R. Lam, D.G. Vlachos, M.A. Katsoulakis, Homogenization of mesoscopic theories, AIChE J., 2002, in press.
[139] J. Liu, M. Xu, F. Zaera, Determination of the rate limiting step in the oxidation of CO on Pt(1 1 1) surfaces, Catal. Lett. 37 (1996) 9.
[140] D.A. Hickman, L.D. Schmidt, Production of synthesis gas by direct catalytic oxidation of methane, Science 259 (1993) 343.
[141] O. Deutschmann, R. Schmidt, F. Behrendt, J. Warnatz, Numerical modeling of catalytic ignition, in: Proceedings of the Twenty Second International Symposium on Combustion, Seattle, Washington, 1996, p. 1747.